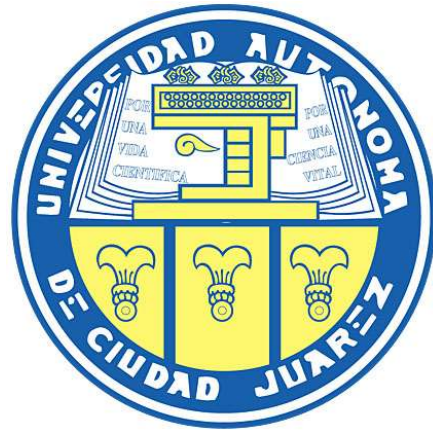# UNIVERSIDAD AUTÓNOMA DE CIUDAD JUÁREZ

INSTITUTO DE INGENIERÍA Y TECNOLOGÍA

DEPARTAMENTO DE INGENIERÍA ELÉCTRICA Y COMPUTACIÓN

FAILURE ANALYIS OF AN ELECTRONIC SYSTEM USED TO RETROFIT A POLARIS GEM E6 FOR AUTONOMY

PROYECTO DE TITULACIÓN

QUE PRESENTA

ALDO URIEL VALENZUELA MORENO

COMO REQUISITO PARCIAL PARA OBTENER EL TÍTULO DE

INGENIERÍA EN SISTEMAS DIGITALES Y COMUNICACIONES

ASESORES

DRA. MARIBEL GÓMEZ FRANCO

DR. JUSTIN RUTHS

CIUDAD JUÁREZ, CHIHUAHUA.   NOVIEMBRE DE 2019

**Title of the Research Project
to which the Technical Report corresponds:**

Retrofitting a Polaris GEM e6 for autonomy.

Type of financing

Institutional – The University of Texas at Dallas

TECHNICAL REPORT TITLE

Failure analysis of an electronic system used to retrofit a Polaris GEM e6 for autonomy.

Authors of the Technical Report:

Aldo Uriel Valenzuela Moreno
Dra. Maribel Gómez Franco
Dr. Justin Ruths

November 11, 2019

Departamento de Ingeniería Eléctrica y Computación

To Whom It May Concern:

It is hereby noted that **C. Aldo Uriel Valenzuela Moreno**, a student at the Universidad Autónoma de Ciudad Juárez in the Digital Systems and Communications Engineering program and enrolment **148865**, made a Research Stay called **Retrofitting a Polaris GEM for autonomy**, in the Mechanical Engineering department of the **University of Texas at Dallas,** from June to July 2019. In the project he was advised by **Dra. Maribel Gómez Franco** teacher of Electrical Engineering and Computer Science department of the Universidad Autónoma de Ciudad Juárez. On the university's part, he was assigned as an advisor to **Dr. Justin Ruths.**

As a result of the research stay it is reported that the project was satisfactory for the **University of Texas at Dallas**. Likewise, the **University of Texas at Dallas** has no problem extending this record so that such a project is used for the aforementioned purposes and grant the facilities for the use of this to the UACJ, in order for the interested party to reach her objective.

Sincerely,

Justin Ruths
Assistant Professor
Departments of Mechanical and Systems Engineering
University of Texas at Dallas
jruths@utdallas.edu

FAILURE ANALYSIS OF AN ELECTRONIC SYSTEM USED TO RETROFIT A POLARIS GEM E6 FOR AUTONOMY

RESUMEN

Siempre existen maneras de mejorar la velocidad, eficiencia y seguridad en vehículos, y la autonomía es una opción extremadamente convincente. Un vehículo eléctrico autónomo es capaz de reducir costos de operación, así como reducir la tasa de incidentes en un 90%. Su tamaño compacto permite que estos vehículos puedan circular más fácilmente en cualquier ruta o terreno, contribuyendo a mejorar el transporte de personal. Además, utilizar este tipo de vehículos contribuye a la reducción de emisión de NOx y ROG, lo cual aborda el actual problema de contaminación en el planeta en general.

La importancia de la investigación *"Retrofitting a Polaris GEM e6 for autonomy"* radica en la reducción de los costos anteriormente mencionados, así como en mejorar la manera en que los estudiantes y profesores se trasladan dentro del campus de UTD. Se estima que una vez que los vehículos autónomos estén disponibles, los estudiantes y profesores reducirán su tiempo de traslado entre edificios, lo cual les permitirá contar con más tiempo para realizar sus actividades académicas. De igual manera, esta investigación busca el reducir los costos de operación, así como los niveles de contaminación en el campus. Además, el campus de UTD se beneficiará al mismo tiempo con el desarrollo de alta tecnología para vehículos autónomos.

En el verano del año 2019, fui participante en el "Programa de Investigación Verano 2019", en *"La Universidad de Texas en Dallas" (UTD)*, en el proyecto de investigación "*Retrofitting a Polaris GEM e6 for autonomy"*, la cual tuvo como objetivo el adaptar un vehículo eléctrico de la marca Polaris GEM, modelo e6, para alcanzar la autonomía, con el objetivo a largo plazo de contar con un sistema de transporte autónomo en la universidad. En esta investigación, llevé a cabo instalaciones, al igual que un diseño sistemático, de componentes electrónicos que serían usados para cumplir el objetivo de la investigación. Instalé sensores de profundidad, cámaras duales, un conmutador maestro, así como una computadora central y una pantalla para monitorear el comportamiento de los componentes. Los resultados obtenidos cuando se realizaron las pruebas de campo, con el objetivo de verificar la funcionalidad de los componentes mientras el auto era conducido, presentaron una falla. Aproximadamente después de 7 a 10 minutos de que el auto había sido encendido (al igual que todos los componentes instalados) y se comenzó a manejar, la

tarjeta *NVIDIA Jetson TX2*, la cual funge como computadora central del sistema electrónico instalado, se apagó.

Debido a esta falla, se plantearon dos teorías acerca del apagado, las cuales consistían en que el circuito estaba solicitando más corriente de lo que la batería podía suministrar, o de lo contrario, existía un sobrecalentamiento en la *Jetson TX2*, debido a que se encontraba colocada en un compartimento sin ventilación. A consecuencia de lo anterior, se realizó el análisis de falla del circuito electrónico.

En este documento se reportan los cálculos, mediciones, así como los resultados obtenidos por las pruebas de funcionalidad realizadas, logrando como resultado, determinar la causa principal de apagado de la computadora central. A partir del análisis llevado a cabo, se pudo determinar que la falla era ocasionada debido al sobrecalentamiento de la *Jetson* TX2, provocado por la falta de ventilación en el compartimento de la misma. A partir de lo anterior, fue propuesto el realizar modificaciones en el compartimento de la *Jetson TX2* con el objetivo de erradicar esta falla.

ABSTRACT

There are always ways to improve speed, efficiency and safety in cars, and autonomy is an extremely compelling option. An autonomous electric vehicle is capable of reducing operating costs, as well as reducing the incident rate by up to 90%. The compact size of these vehicles makes them circulate more easily on any route or terrain, contributing to improve personnel transport. In addition, using this type of vehicle contributes to the reduction of NOx and ROG emissions, which addresses the current problem of pollution on the planet in general.

The importance of the research *"Retrofitting a Polaris GEM e6 for autonomy"* lies in the reduction of the aforementioned costs, as well as the improvement of the way students and teachers move within the UTD campus. It is estimated that once autonomous vehicles are available, students and teachers will reduce their transfer time between buildings, which will allow them to have more time to carry out their academic activities. In the same way, this research seeks to reduce operating costs and pollution levels within campus. Also, the UTD campus will benefit at the same time with the development of high technology for autonomous vehicles.

In Summer 2019 I was a participant in the UT Dallas-Mexico Summer Research Program 2019 at *The* University *of Texas at Dallas (UTD),* in the research project "*Retrofitting a Polaris a GEM e6 for* autonomy". This had as an objective to adapt a Polaris GEM e6 electric vehicle, to lead to autonomy, with the long-term goal of an autonomous university transport system. I carried out a systematic design and installation of electronic components to be used to fulfill the objective of the investigation. I installed depth sensors, dual cameras, an electrical switch, as well as a central computer and a screen to monitor the behavior of the components. The results obtained when performing field tests, in order to test the functionality of the components when the car was driven, were performed, and a failure occurred. Approximately 7 to 10 minutes after the car had been started (and all the components were running) and it began to drive, the Jetson TX2, which serves as the central computer of the installed electronic system, turned off.

Due to this failure, a failure analysis of the electronic system was performed. Two theories were raised about the shutdown; either the circuit was requesting more current than the battery could supply, or on the other hand, there was an overheating on the Jetson TX2, caused by its location. The Jetson TX2 was placed in a compartment without ventilation.

Calculations and measurements are reported in this document, as well as results obtained by functionality tests performed. On consequence, it was possible to determine the root cause of the shutting down problem of the central computer. Due to this, the failure found in the initial functionality tests could be solved. It was proposed to perform modifications to the compartment of the Jetson TX2 in order to eradicate this failure.

STATEMENT OF ORIGINALITY

I hereby declare that to the best of my knowledge, the material contained in this document is my own work. This document is original and has not been copied from any other source, nor has it been used to obtain another degree or recognition at another institution of higher education.

I certify that the intellectual content of this document is the product of my own work on all the assistance received in preparing this technical report and sources have acknowledged.

Aldo Uriel Valenzuela Moreno

KEYWORDS

Failure Analysis, Autonomous vehicle, Velodyne LiDAR, ZED Camera, Polaris GEM.

POTENTIAL USERS

This research project seeks to explore the idea of using autonomous vehicles to eventually serve as public transportation around to the UTD campus, benefiting specially to students and UTD personal.

ACKNOWLEDGMENTS:

Contents

LIST OF FIGURES

LIST OF TABLES

1   INTRODUCTION

Driving, for over a hundred years, has been exclusively an activity that only humans were able to perform. Nevertheless, it has been determined that in 93% of total crashes per year in the United States, the human error is the primary factor. There are more than 32,367 fatal crashes per year in the U.S, where 31% of fatal crashes involving alcohol and 21% involving a distracted driver, lashing out, again, human error [1].

In most metropolitan areas, cars and trucks are the major source of air pollution. A legitimate example of this is California, where on-road mobile sources are responsible for 51% of nitrogen oxides (NOx) and 33% of reactive organic gases (ROG) emissions, both ozone precursors [2]. This pollution has been caused by vehicles that depend solely on petroleum-derived fuels, such as gasoline and diesel.

According to the article "*Preparing a nation for autonomous vehicles: opportunities, barriers and policy recommendations*" published by Daniel J. Fagnant and Kara Kockelman [1] over the past few years the automobile and technology industries have made significant leaps in bringing computerization into what has, for over a century, been exclusively a human activity, driving. Autonomous vehicles (AVs) represent a potentially disruptive yet beneficial change to our transportation system. This new technology has the potential to impact vehicle safety, traffic congestion, and travel behavior. All told, major social AV impacts in the form of car crash savings, travel time reduction, fuel efficiency and parking benefits are estimated to reach $2000 per year per AV, and may eventually reach nearly $4000 when comprehensive car crash costs (combination of tangible impacts and the monetized pain and suffering [3]) are accounted for.

Each year, it is estimated that there are approximately 272 million vehicles in operation on the United Stated roads [4]. Car accidents have a very high cost due to injuries and time, as well as fuel, which are wasted by people trapped in traffic jams generated by such accidents. It has been determined that human error is the main factor in 93% of all accidents [1], which means that autonomous vehicles could have a huge positive impact on the aforementioned costs.

"Transportation has been one of the largest sources of air pollution produced by human activity in the United States" [5]. Focusing in the United States, more specifically in its two largest contiguous states (Texas and California), in 2017 more than 23 million vehicles were registered

[6]. Having this incredible number of vehicles (just in two states), without a doubt, contributes to pollution in the United States, and therefore, contributes to pollution in our planet.

Focusing on the UTD (*The University of Texas at Dallas*) campus, it has been observed that, as the campus continues to expand, students, as well as teachers, must travel longer distances to take or teach their respective lectures, often in extreme temperatures. Similarly, due to schedules and distances, some students have very little time to move from one side of the campus to the other, making it difficult for them to be punctual in their activities.

The internal transportation system of the university has areas of opportunity that can be addressed, such as the reduction of operating costs, the improvement of routes, both in infrastructure and expansion of these, and mainly, the reduction of transfer time.

The main objective of the main project is to build an electric vehicle research platform to study problems related to the security of controlled and automated systems, in order to analyze the idea of having, in the future, an autonomous transport system on UTD campus. Therefore, this research project seeks to collaborate with the "Environmental Affairs" from UT Dallas, which "maintains and updates the University's air permit authorizations, tracks emissions sources, determines permit applicability, and prepares permit applications" [7]. My collaboration in this research was based on the technical part, which had the specific objective of integrating all the components (interconnections and installations) into the car, to enable monitoring its behavior; test their functionality and prepare everything (referring to the technical part) to continue to the next phases.

When the functionality tests were performed, a failure occurred. Due to this problem, a failure analysis of the electronic system was proposed. This analysis had the purpose of identifying the root cause of the failure, in order to solve the problem and propose a solution to prevent this malfunction occurring again.

The performance of the failure analysis was successful, since the root cause could be determined and an implementation, in order to solve and prevent this failure, was proposed and performed, getting as results the eradication of the original failure.

2 PROBLEM STATEMENT

Project background

Retrofitting a Polaris GEM e6 for autonomy

The idea of having autonomous public transportation has been an area of interest for both public and scientific community for a while now.

Dr. Justin Ruths, a UTD assistant professor in Mechanical Engineering and Systems Engineering departments, who spans his work "across the topics of control, dynamics, computation, optimization, and networks" [8], proposed the project research *"Retrofitting a Polaris GEM e6 for autonomy"*, which has the following structure (Figure 1).

Figure 1. Project research structure.

In 2018, a team of mechanical engineers, worked in the mechanical phase. They were focused in researching, creating and buying the components to be used in the research project. After they made their research, in their selection, they included two sensor types: LiDAR sensors, which use infrared light, and 3-D cameras for visual depth perception. Also, they considered necessary an NVIDIA Jetson TX2 board as well as a monitor to visualize the behavior of the components [9]. These items will be explained in the *"Theoretical framework"*.

After their selection, they made some designs and tests of the components, where they got the following results. Some of their results are shown in the following figures (Figures 2 - 4).

The Velodyne LiDAR sensor was configured and mounted successfully with the addition of a metal arm to ensure its safety in case of danger of theft.

- Correct configuration of the sensor and proper operation.
- Proper camera mounting and operation.

Figure 2. Velodyne LiDAR sensor mounted with securement bracket.

Figure 3. ZED camera mounted.

Figure 4. LiDAR functionality test, [9].
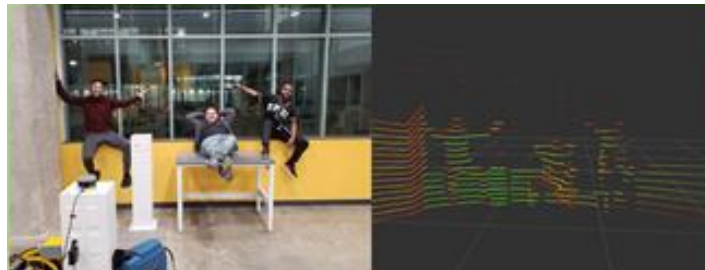
In 2019, a team of informatics engineers got involved in the computing phase. Their contribution consisted on gathering the data from the sensors, displaying the data on a dashboard user interface, and logging the data to an SQL database [10]. They separated their phase into three separate programs (Figure 5). They achieved to develop the following programs.

- Core program
  - o Responsible for collecting data from sensors.
  - o Shares collected data to other programs.
- Data logging program
  - o Receives data from core program.
  - o Stores data locally until a connection to the server is made.

- o Uploads data to a MySQL server.
- UI Program
  - o Receives data from core program.
  - o Displays relevant data to user.
  - o Uses QT library for GUI code.

These three programs together provide the user the opportunity of monitoring the behavior of the components connected to the Jetson TX2.

Figure 5. Structure of the three programs, [10].
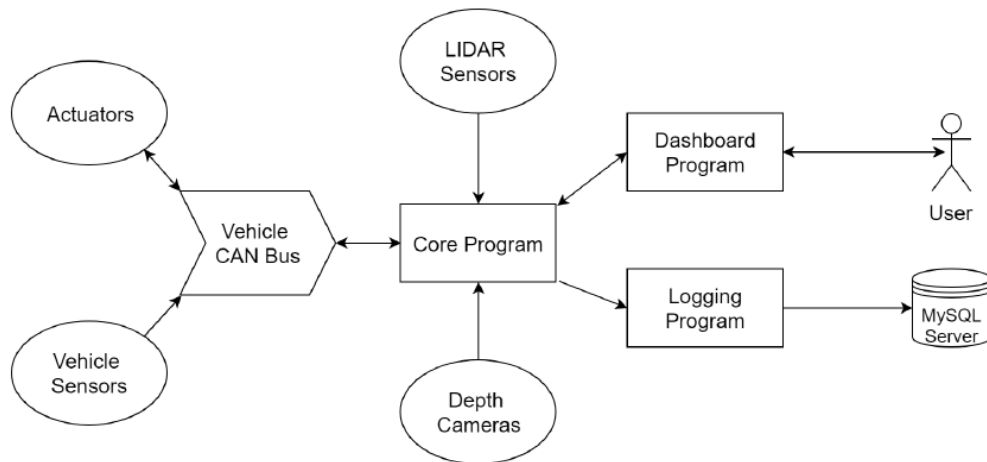
With the results obtained it was considered that the research project completed the mechanical and computing phases. This gave way to the next phase, the technical phase.

Failure analysis of an electronic system used to retrofit a Polaris GEM e6 for autonomy.

The technical phase was focused on the installation and interconnection of components such as depth sensors, dual cameras, an electrical switch and a central computer, as well as a screen to monitor the behavior of the components. Once this phase reached the field tests part, a failure occurred. Approximately 10 minutes after the car had begun to be driven, the central computer shut down.

Due to this failure, in order to find the root cause of this failure and, solve the problem, a failure analysis of the electronic system was proposed.

Theoretical framework

Literature review

According to J. Rooney and L. Vanden, a "root cause analysis (RCA) is a process designed for use in investigating and categorizing the root causes of events with safety, health, environmental, quality, reliability and production impacts" [11]. This tool is helpful for identifying what, how and why an event happened, thus preventing recurrence. An event could be defined as an occurrence that produce or has the potential to produce the impacts mentioned above. The RCA is a process that involves data collection, root cause identification and recommendation to solve and prevent the failure analyzed.

A quick overview of the steps should be followed to conduct an RCA is given by the "Guidance for Performing Root Cause Analysis (RCA) with Performance Improvement Projects (PIPs)" [12], which is shown in the Table 1.

Table 1. Steps to conduct RCA, [12].

Steps	Explanation
1. Identify the event to be investigated and gather preliminary information	Events and issues can come from many sources (e.g., incident report, risk management referral, resident or family complaint, health department citation). The facility should have a process for selecting events that will undergo an RCA.
2. Charter and select team facilitator and team members	Leadership should provide a project charter to launch the team. The facilitator is appointed by leadership. Team members are people with personal knowledge of the processes and systems involved in the event to be investigated.
3. Describe what happened	Collect and organize the facts surrounding the event to understand what happened.
4. Identify the contributing factors	The situations, circumstances or conditions that increased the likelihood of the event are identified.
5. Identify the root causes	A thorough analysis of contributing factors leads to identification of the underlying process and system issues (root causes) of the event.
6. Design and implement changes to eliminate the root causes	The team determines how best to change processes and systems to reduce the likelihood of another similar event.
7. Measure the success of changes	Like all improvement projects, the success of improvement actions is evaluated.

The 8D methodology is a tool to solve problems that involves team working, using a structured 8 step approach to help focus on facts. C. Riesenberger and S. Sousa indicate that once a problem has been recognized, 8 disciplines (8D) are used to solve it. "The 8D steps are: D1-team formation; D2-problem analysis; D3-containment actions; D4-root cause analysis; D5-corrective actions; D6-verification of the effectiveness of the corrective actions; D7-preventive actions; D8-congratulate

the team" [13]. However, the 8D is not effective for non-recurring problems or problems which can be solved quickly by individual effort. Although, this does not mean that some of its disciplines are not useful. The use of this tool is under consideration of the user.

Focusing on the topic of the main research project, a troubleshooting was performed in [14]. The team analyzed the anti-blocking system (ABS). Wires connected to ABS electronic control unit (ECU) had failures. Considered defects included, for instance, broken plug-connectors, broken wires, shorted to ground or battery wires, stuck switches, etc. Then, it was shown a dialogue proposed that showed how, starting from an observed symptom, MDS ("a tool that implements model-based engineering for various tasks related to the analysis of the behavior of a product when failures are present.") proposes control-actions to transition the system in useful states, and measurement actions to discriminate among possible diagnoses. The dialogue is composed of 6 steps, which can be reduced to: observation, proposing, testing, measuring. To solve the identified problem, they observed what was wrong and proposed a solution. Once the solution was implemented, they performed tests and they realized that their proposed solution was successful. Finally, they measured voltage and resistance to compare their results against the expected values.

Converging on the shut down failure, it was found the "Measurements Analysis of the Software-Related Power Consumption in Microprocessors" [15], where it was stated that "the energy consumed during the execution of instructions can be distinguished in two components. The base cost, energy amount needed for the execution of the operations which are imposed by the instructions, and the inter-instruction const which corresponds to an energy overhead due to the changes in the state of the processor provoked by the successive execution of different instructions". This analysis offers relevant data about how the power behaves in a microprocessor.

Continuing with the microprocessor and power consumption, in [16] it was exposed that power consumption in high-performance microprocessors has increased with successive generations. Also, in [17] it was exposed that "in the design of modern processors, power and thermal management have become prominent issues of portable computer systems". To face these issues, in the report "Using DTVS Technique for Microprocessor's Power and Thermal Management" it was proposed the *Dynamic threshold voltage scaling* (DTVS) technique, which is an effective low-power design technique for reducing the dissipated power. Results on this report it was shown that a significant amount of power consumption alterations were occasioned by different workload environments.

Conceptual framework

The electrical scheme shown in Figure 6, is a representation of a parallel circuit. According to Robert L. Boylestad in his book "Introductory Circuit Analysis" [18], the voltage in the parallel elements is the same. And, for parallel networks of a single source, the source current (I_s) is equal to the sum of the individual branch currents. These statements can be justified by the following equations.

Figure 6. Parallel circuit scheme.
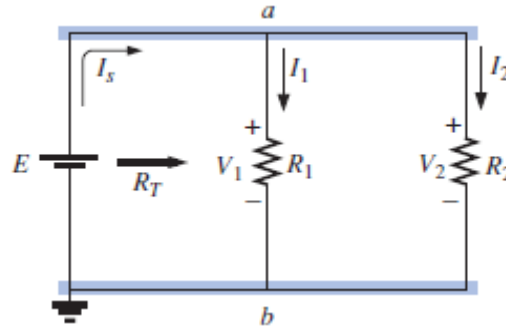
$$E = V_1 = V_2 \tag{1}$$

$$I_s = I_1 + I_2 \tag{2}$$

Also, according to Kirchhoff's current law (shown in the book previously mentioned), the total current entering a circuits junction is exactly equal to the total current leaving the same junction. This statement is expressed with the following equation.

$$\sum I_{in} = \sum I_{out} \tag{3}$$

According to S. William and Z. Li, in their book "Electricity Generation Using Wind Power" [19] "the power of a system is the time rate of doing work or expending energy and therefore has the dimension of energy (W or work) divided by time". For large increments of time t, the average power P is given by:

$$P = \frac{W}{t} \tag{4}$$

In the *Système Internationale* (S.I.) the unit of energy is the joule and the unit of power is the joule per sec (J/s), which is usually referred as the watt (W).

In [20] it is stablished that "the difference in potentials between two points is equal to the energy peer unit charge and this is required to move electric charge between the points, as we

know, electric current measures the charge per unit time (in coulombs/second). The electric power P is given by the product of the current I and the voltage V". This expression is shown in the following equation.

$$P = IV$$ <div align="right">(5)</div>

The equations 4 – 5 are some of the quantitative form of Joule's law.

Following, with the purpose of knowing the components used in this research project, these are briefly explained.

Component description
Polaris GEM e6

According to the Polaris company webpage [21], "GEM e6 is the ideal people mover. It has enhanced suspension that trails over rough terrain without compromising comfort. GEM e6 is perfect for moving people around campus, across town and around the local community". This electric vehicle is shown in the Figure 7.

Figure 7. Polaris GEM e6, [21].

Some of its outstanding specifications and features are shown in Table 2. This information can be found in the Appendix A.1

Table 2. Polaris GEM e6 specifications.

Specifications	
Battery Range	12-68 mile; dependent on battery type
Battery Type	Lithium-Ion of 12.4 kWh
Engine Type	48V AC Induction Electric
Horsepower	8.7 HP (6.5 kW-h)
Top Speed	25 mph

Velodyne LiDAR PUCK

According to the datasheet of the Velodyne LiDAR PUCK (VLP-16), which can be found in the Appendix A.2, this sensor "is the smallest, cost-optimized product in Velodyne's 3D LiDAR product range". The VLP-16 has a range of 100 meters, and the sensor's low power consumption, light weight, compact footprint and dual return capability make it ideal not only for autonomous vehicles but also for robotics, terrestrial 3D mapping and many other applications (Appendix A.2). Some of its outstanding specifications are shown in Table 3. An image of this sensor is shown in the Figure 8.

Table 3. Velodyne LiDAR PUCK specifications.

Specifications	
Sensor	Measurement Range: 100 m
	Field of View (Vertical): +15.0° to -15.0° (30°)
	Angular Resolution (Vertical): 2.0°
	Field of View (Horizontal): 360°
Mechanical/ Electrical/ Operational	Power consumption: 8 W (Typical)
	Operating Voltage: 9 V - 18 V
	Operating Temperature: -10°C to +60°C
Output	Single Return Mode: ~300,000 points per second
	Dual Return Mode: ~600,000 points per second

Figure 8. Velodyne LiDAR PUCK, [22].
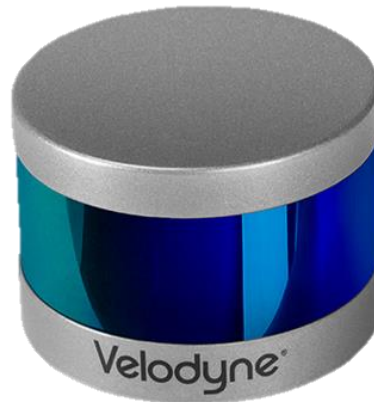
ZED camera

The ZED (Figure 9) is a camera that reproduces the way human vision works. Using its two "eyes" and through triangulation, the ZED provides a three – dimensional understanding of the scene it observes, allowing an application to become space and motion aware.

Depth perception is the ability to determine distances between objects and see the world in three dimensions, the ZED camera is the first universal depth sensor. According to the datasheet of this component (Appendix A.3), some of its outstanding specifications are shown in Table 4.

Figure 9. Zed camera, [23].

Table 4. ZED camera specifications.

Specifications	
Output Resolution	Side by Side 2x (2208x12412) @ 15fps
	2x (1920x1080) @30fps
	2x (1280x720) @60fps
	2x (640x480) @100 fps
Depth range	1 m to 15 m (3.5 to 49 ft)
Power	380mA / 5V USB Powered
Operating Temperature	0°C to +45°C (32°F to 113°F)

NVIDIA Jetson TX2

According to the developer Nvidia website [24] the "Jetson TX2 is the fastest, most power-efficient embedded AI computing device. This 7.5-watt supercomputer on a module brings true AI computing at the edge. It's built around an NVIDIA Pascal™-family GPU and loaded with 8GB of memory and 59.7GB/s of memory bandwidth. It features a variety of standard hardware interfaces that make it easy to integrate it into a wide range of products and form factors". Some of its outstanding specifications are shown in Table 5. An image of this component is shown in Figure 10. Specifications for this component can be found in the Appendix A.4.

Table 5. NVIDIA Jetson TX2 specifications, [24].

GPU	256-core NVIDIA Pascal™ GPU architecture with 256 NVIDIA CUDA cores
CPU	Dual-Core NVIDIA Denver 2 64-Bit CPU Quad-Core ARM® Cortex®-A57 MPCore
Memory	8GB 128-bit LPDDR4 Memory 1866 MHx - 59.7 GB/s
Storage	32GB eMMC 5.1
Power	7.5W / 15W

Figure 10. NVIDIA Jetson TX2, [24].
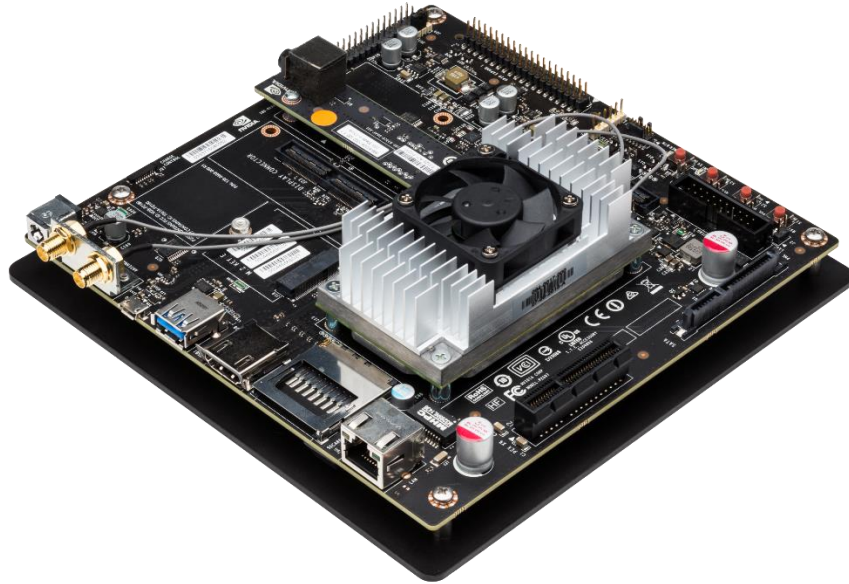
Anker USB Hub

The Anker USB 3.0 13-port (Figure 11), according to its "Welcome Guide" (Appendix A.5), it is a hub that easily add 13 USB 3.0 ports to any compatible system and eliminate the hassle of having to switch between devices. Also, it ensures a stable power supply while working. The solid aluminum body ensures its usage for years. It includes a 12V 5A power adapter (10ft). Table 6 shows its main specifications.

Figure 11. Anker USB Hub, [A.5].

Specifications	
Data Port Output Current	0.9 A
Charging Port Output Current	2.1 A
Input Interface	USB 3.0 type B
Output Interface	13 type A USB 3.0 ports with maximum speeds of up to 5Gbps, 1 type A Smart Chargin Port with output current of 2.1A

GeChic On-Lap 1102I Touchscreen Monitor

According to the GeChic website [25], the "1102I, a 11.6" touch monitor with FHD and wide-viewing angle, is designed as performance-focused transformer. The 1102I uses Projected Capacitive Touch technology to deliver a more sensitive, accurate 10-point multi-touch". Also, this monitor combines the advantages of FHD, 16.7M true color, high contrast ratio and fast response time, allowing reading webpages, viewing photos, watching videos with more crystal clear, sharper image quality on a more power-saving screen. Table 7 shows its main specifications. This information can be found in the Appendix A.6. An image of this component is shown in the Figure 12.

Table 7. GeChic On-Lap 1102I Touchscreen Monitor specifications.

Specifications	
Panel	11.6" (16:9 Wide)
Resolution	1920x1080
Color Depth	16.7M Colors
Viewing Angle	178°(H)/178°(V)(CR>10)
Touch Points	10 detections
Rating Power	5V --- 1.7A
Operating Temperature	0°C to 50°C

Figure 12. GeChic On-Lap 1102I Touchscreen Monitor, [25].

3 METHODOLOGY

The development of the research project "Retrofitting a Polaris GEM e6" was performed used the following diagram (Figure 13). Focusing on the first stage, the activities performed can be observed in the diagram shown in the Figure 14.

Figure 13. Methodology diagram.
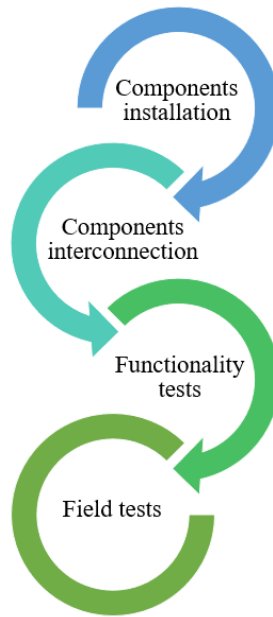
Figure 14. Components installation stage.
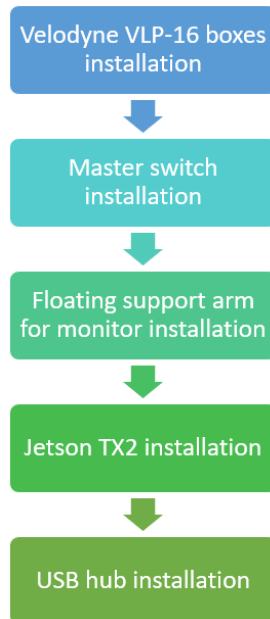
In order to complete these stages, the following activities were performed.

Before starting the components installation stage, the location of these components was proposed as it is shown in Figure 15.

Figure 15. Location of components.
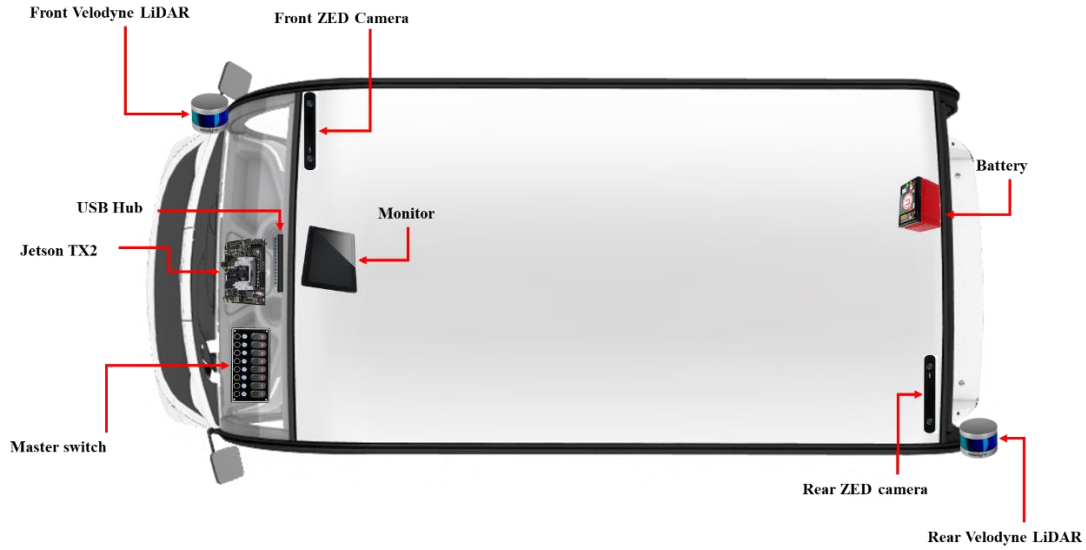
Once the location of components was determined, the installations were performed.

The first installation that was made, was the VLP-16 boxes installed in the front part of the car, an evidence of this is shown in the Figure 16. Once this was installed, the interconnection between the VLP-16 boxes and the VLP-16 sensor was made through the interior of the car with 13.5-foot, 12-gauge cables. Specifications of the wire used, can be found in the Appendix A.7.

Figure 16. Front Velodyne Lidar VLP-16 box installed.

Then, the dashboard, as well as the steering wheel and the handbrake, were removed. The top dashboard was pierced with the purpose of being able to place the electrical switch inside of it. To perform this activity a reciprocating saw was used. Once this activity was done, the electrical switch was placed inside of it, as can be observed in the Figure 17.

Figure 17. Electrical switch installation.

After some designs and proposals about the monitor location, removing the central rear view was decided. Once this was removed, instead of the central rear view, a combination of two different pieces (Figures 18-19) were performed, with the purpose of installing a floating support arm for the monitor. The result of this installation can be observed in the Figure 20.

Figure 18. Monitor holder number one.

Figure 20. Floating support arm installation.

Again, in the top dashboard was installed another component, the Jetson TX2. This component was placed inside of a compartment that the dashboard already included, it fitted perfectly. There was necessary drill some holes in the front part to collocate the cables through into. This installation can be observed in the Figure 21.

Figure 21. Jetson TX2 Installation.

Finally, the last installation made was the USB hub one. This USB Hub was placed inside of the front dashboard. The achievement of this stage, allowed to continue with the next stage, the interconnection of the components. The USB Hub installation is shown in the Figure 22.

After the USB Hub installation, the top dashboard was installed back (Figure 23). Once all the components were placed, interconnections between them were made. This involved connecting the USB Hub, the Jetson TX2 and both Velodyne Lidar into the electrical switch (Figure 24). Three wireless keyboards, two Zed cameras, two cables corresponding to the monitor, and two cables, just for communication, for Velodyne Lidar VLP-16, were connected into the USB Hub, as was shown in the Figure 22. The inner interconnection and organization of cables of the car and the electronic system is shown in the Figure 25.

Figure 23. Top dashboard installed back.
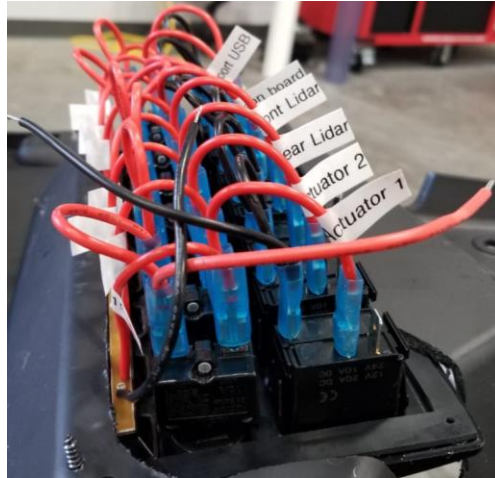
Figure 25. Inner interconnection and installation.

The Figures 26-28 show what the car looked like once all connections and installations were made. Also, the Figures 29-31 show what the car looked like after all the installations and connections were performed, showing the VLP-16 sensors and the ZED cameras outside the car. After these connections and installations, functionality tests were performed.

Figure 26. Front view of the interior of the car.

Figure 27. Left view of the interior of the car.

Figure 28. Right view of the interior of the car.

Figure 29. Front view of the car.

Figure 30. Side view of the car.

Figure 31. Rear view of the car.

To perform the functionality tests, all the components were connected and turned on. All the components worked correctly, as it is shown in the following figures (Figures 32 – 37).

Figure 33. USB Hub on.

Figure 34. Jetson TX2 on.
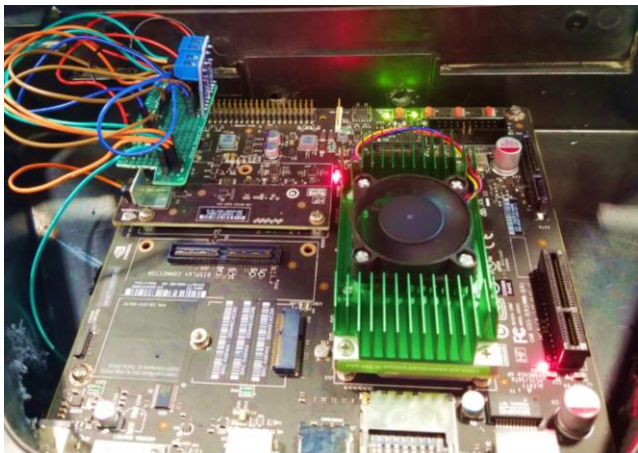
Figure 35. Zed camera on.
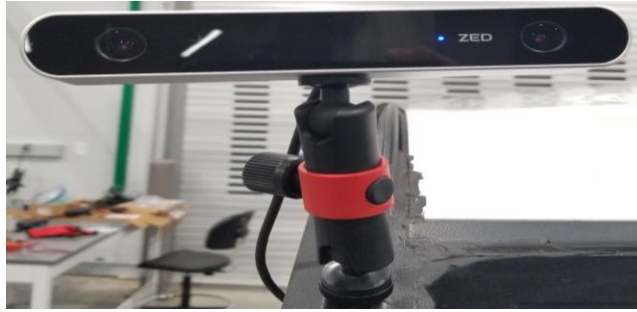
Figure 36. Velodyne Lidar VLP-16 on.

Figure 37. Monitor on.
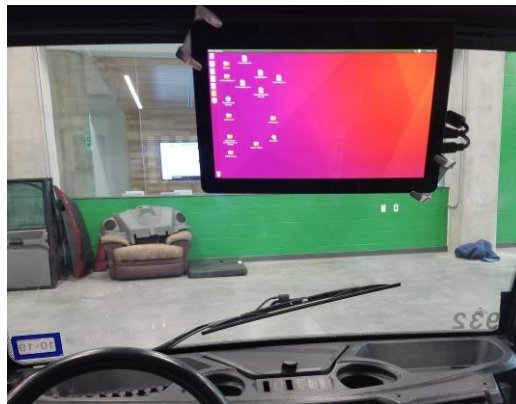
With these stages finished, the following electrical scheme (Figure 38) was proposed. This electrical scheme was proposed with the purpose of representing the electronic system connections. Notice that the red lines indicate data communication. In Figure 38, can be observed that the battery is connected to a switch, which is connected to a USB Hub, a CPU (Jetson TX2), two VLP-16 and two actuators. Also, it is shown that in the USB Hub there are connected three Bluetooth keyboards, a monitor (power supply and touchscreen) and both VLP-16. The VLP-16 connections are just for data communication.

Figure 38. Electrical scheme for electronic system connections.
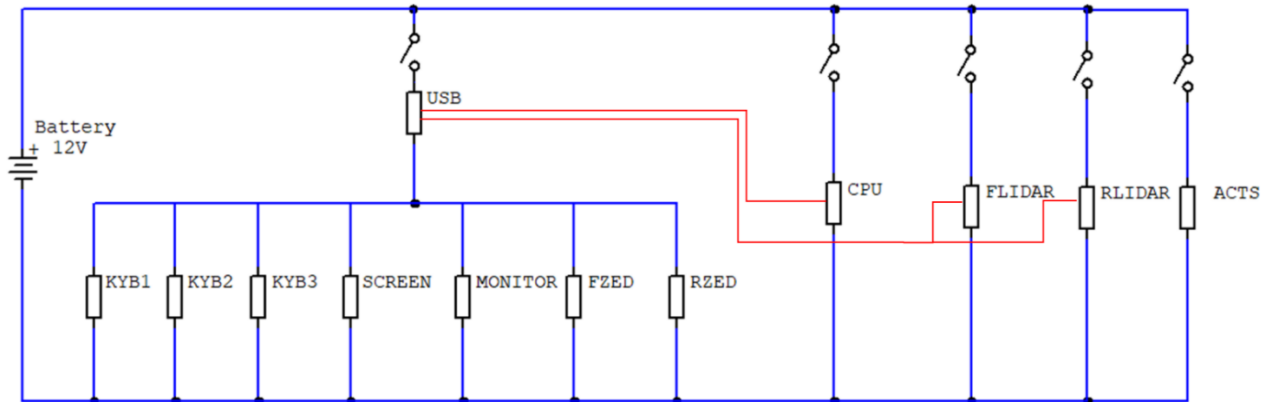
To finalize the stage of the proposed methodology, field tests were performed. These tests consisted of driving the car across the campus with all the components on. However, two errors were found. The first one was about the software (created by the informatics engineers' team), more specifically in the VLP-16 viewing section. When the car was been driven, the images shown in the monitor, corresponding to the VLP-16 lidars were not clear. The images consisted in many purple dots instead of representing the real scenario. This error can be observed in the Figure 39.

Figure 39. Erroneous representation of depth.

Due to this failure was about the software, corresponding to the computing phase, it was decided that the solution to this would be beyond the scope of this technical report. However, in the results section, there are shown some images obtained with the VLP-16 and ZED using their respective default software instead of the one developed by the informatics engineers' team.

The second failure was that, after approximately 7 to 10 minutes that the car had begun to be driven, the Jetson TX2 turned off. Due to this failure, this "Failure analysis for an electronic system used to retrofit a Polaris GEM e6 for autonomy" was performed.

Based on the methodologies, techniques and tools for problem solving and root cause analysis, shown in the *theoretical framework* section, it was proposed to adapt them and use a new

methodology. The objective of this was to solve the problem found, finding the root cause of the failure.

As result of the above, the failure analysis shown in the *Results* section was performed. To perform this failure analysis, the electrical scheme for electronic system was modified as it is shown in Figure 40.

Figure 40. Electrical scheme for components in vehicle.
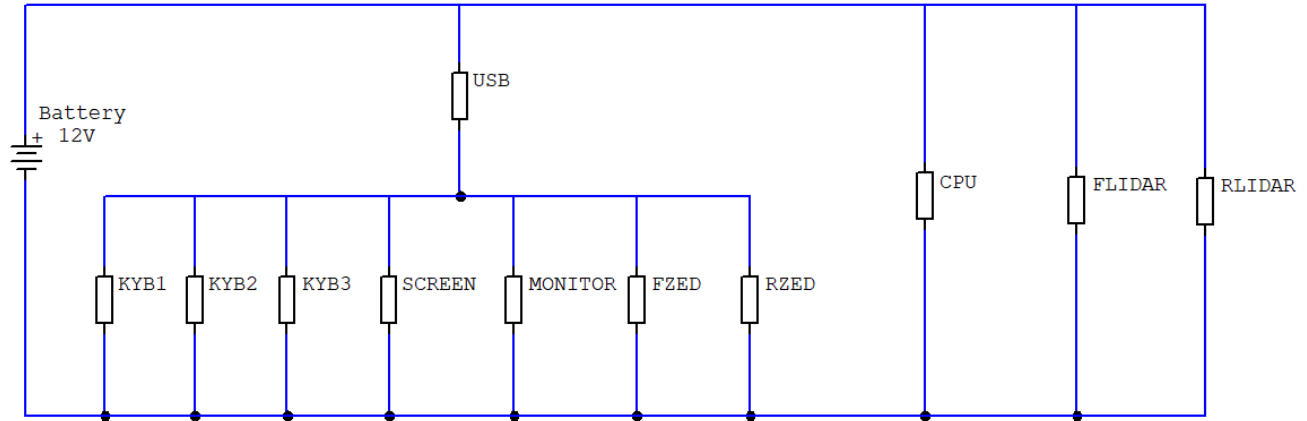
Tests scenarios and equipment used

In order to compare the results obtained by the calculations with the nominal values, and the "real" values (values obtained when measurements are performed), it was proposed different scenarios to perform field tests.

The first scenario consisted of using a "truth table" structure. In this structure, it was performed some combinations (in this case, there were 16 combinations) in order to measure current and voltage in different locations in the electronic system. The measurements were performed in the battery, the switch and in each terminal of the components. The equipment used to perform this activity, were two multimeters.

The voltmeter used to measure voltage was the "True RMS Multimeter Extech 411A" which has 8 different actions and +/-0.5 percent basic accuracy. Further information can be found in the Appendix A.8.

The ammeter used to measure current was the "400 AC/DC Clamp meter CL380" which has automatically ranging True Root Mean Squared (TRMS) measurement technology for accuracy. Further information can be found in the Appendix A.9.

The second scenario consisted of driving the car, with the top deck of the dashboard opened. The stage for driving the car was the first floor of a covered parking lot. Driving the car, in this test, required turning on all the components. Video recording was an activity performed in this test, in order to record the behavior of the VLP-16 and the ZED cameras.

To perform this test, it was necessary driving the same circuit twice. This was due to the software failure previously shown. This failure made it impossible to record the front (VLP-16 and ZED cameras) and rear behavior at the same time. Driving the circuit twice allowed to record the behavior of the car components.

4 RESULTS

As it was shown before, there was a problem on regard of the computer shutting down. To figure out what the main factor of the shutdown was, two theories were planted.

➢ **Theory number one:** The Jetson TX2 required more current than battery can supply, thus causing it to shut down once it did not receive the required current.

➢ **Theory number two:** The Jetson TX2 was overheating, causing it to shut down as a security measure.

In order to fix this issue, starting from theory number one, the following calculations were made.

Calculations and analysis regarding theory number one

According to the electrical scheme shown in Figure 6, as well as equations 1-2, it is possible to reduce the original electrical scheme shown in Figure 40, to the electrical scheme shown in Figure 41. Also, using the equation 3, expressed by Kirchhoff's current law, the electrical scheme can be reduced as shown in the Figure 42.

Figure 41. Electrical scheme reduction.
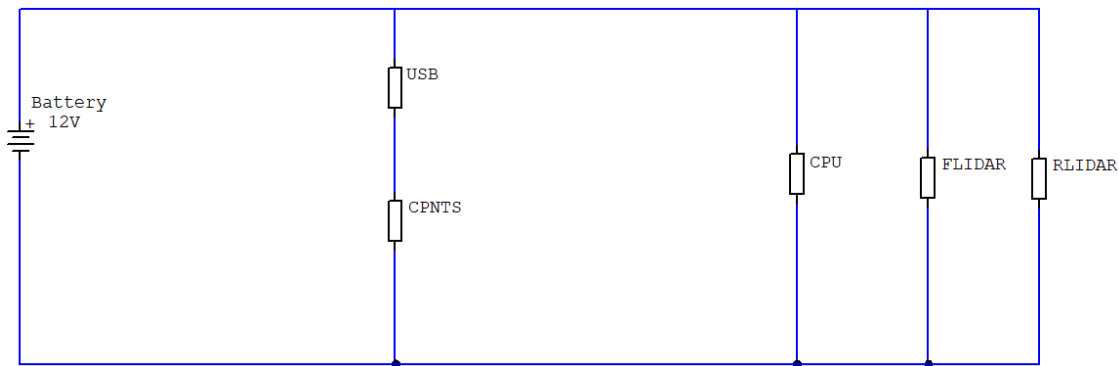
Figure 42. Final electrical scheme.
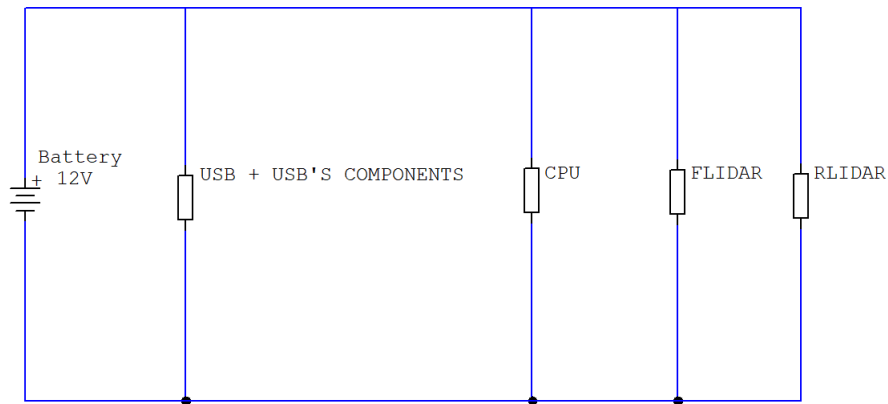
The following calculations were made using the electrical diagrams shown above, based on the electrical scheme shown before (Figure 42), considering different operating conditions. All the datasheets and technical specifications can be seen in the Appendix A (A.1-A.6).

Finally, remembering that theory number one suggested that the current required by the CPU and the whole circuit was not enough, the following calculations were made in order to find the total current consumption of the circuit, as well as that of the branch of the CPU, based on the diagram shown in Figure 43.

Figure 43. Final electrical scheme with currents.
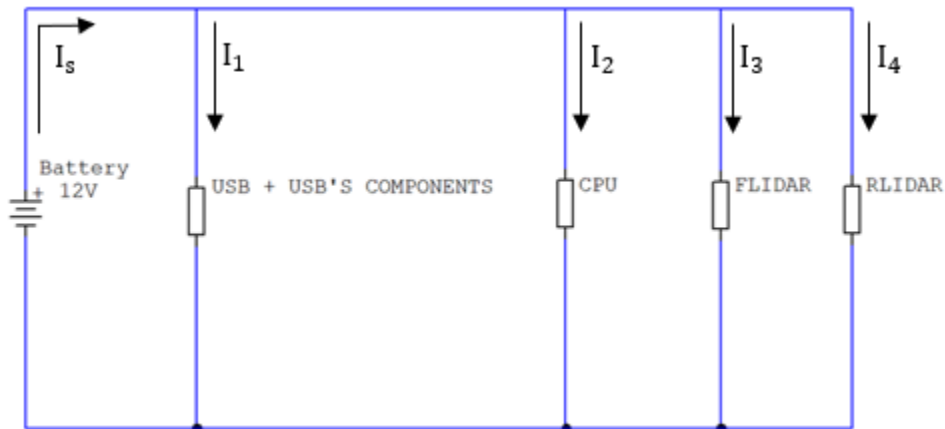
1. Considering all the components working at maximum power.

Table 8 shows the maximum values that were considered to perform the first calculation. (values obtained from Appendix A.2 - A.5)

Table 8. Considering all the components working at maximum power.

Component	Voltage (V)	Power (W)	Current (A)	Current number
USB HUB	12	96	8[*1]	I_1
Jetson TX2	12	90[*2]	7.5	I_2
Front LiDAR	12	8	0.67	I_3
Rear LiDAR	12	8	0.67	I_4

[*]Note 1: In the Appendix A.5 it is stated that for maximum performance, connected devices should not exceed a combined current of 8 A.

[*]Note 2: This value has been set as the maximum power, however, there was no certain information about this value. Because of this, more calculations were performed, considering all the power consumption values found.

Using equation number two shown above, the following calculation was made.

$$I_S = I_1 + I_2 + I_3 + I_4 \tag{6}$$

$$I_S = 8\,A + 7.5\,A + 0.67\,A + 0.67\,A = \mathbf{16.84\,A} \tag{7}$$

However, as the table's note establishes, the current could be of maximum 8 A. This would be considering that the sum of the current of each port (having 13-port of 0.9 A and 1-port of 2.1 A). Nevertheless, 7 ports of 0.9 were being used. Considering this, the calculation changed as follows.

$$I_1 = 0.9\,A + 0.9\,A + 0.9\,A + 0.9\,A + 0.9\,A + 0.9\,A + 0.9\,A = \mathbf{6.3A} \tag{8}$$

$$I_S = 6.3\,A + 7.5\,A + 0.67\,A + 0.67\,A = \mathbf{15.14\,A} \tag{9}$$

Notwithstanding, continuing with the USB current consideration, according to the components connected in the 7-port, and according to the Figure 44 obtained from the datasheet of the USB HUB (Appendix A.5), as well as with the datasheet of the ZED cameras (Appendix A.3), the following calculation was made.

Figure 44. USB Hub specifications.

Mouse	100mA
Camera	>300mA
Portable hard disk	max. 500mA
USB 3.0 portable hard disk	max. 900mA
Keyboard	max. 500mA

$$I_1 = 0.5\,A + 0.5\,A + 0.5\,A + 0.38\,A + 0.38\,A + 0.9\,A + 0.9\,A = \boldsymbol{4.06A} \tag{10}$$

$$I_s = 4.06\,A + 7.5\,A + 0.67\,A + 0.67\,A = \boldsymbol{12.9\,A} \tag{11}$$

This result hints that the current required by the whole circuit, due to the current required by the Jetson TX2, was not enough. Remembering that the battery could supply 12 volts and 12 amperes, the whole circuit required 0.9 amperes more than the battery could supply.

However, using the information shown in the note number two, more calculations were proposed. The following calculations were made using the last current calculated for the USB HUB and different values for the Jetson TX2 power.

2. Considering 55.1 watts as the power dissipated by the CPU

According to the datasheet for the Jetson TX2 (Appendix A.4), the supplied power is rated to 90 W. This information was used in the last calculation. However, the main power input from DC adapter is considered using 19.6 V. In the circuit that it was being use in this research project, the power supply was of 12 volts. Therefore, using the Rule of Three with the values above, the power consumption for the Jetson TX2 was calculated as follows.

$$19.6\,V - 90\,W \tag{12}$$

$$12.0\,V - X$$

$$X = \frac{(12.0\,V \times 90\,W)}{19.6\,V} = 55.1\,W \tag{13}$$

Using the following equation, based on equation 5, the current can be calculated.

$$P = VI \ \therefore I = \frac{P}{V} \tag{14}$$

Where:

P = Power (watts)

V = Voltage (volts)

I = Current (amperes)

Considering 12 volts (the voltage supplied by the battery), the current for the Jetson TX2 would be:

$$I = \frac{P}{V} = \frac{55.1\,W}{12\,V} = 4.59\,A \tag{15}$$

With this result, the values used to perform the calculation with 55.1 watts, are shown in Table 9. With these values, the following calculations were made.

Table 9. Considering 55.1 watts as the power dissipated by the CPU.

Component	Voltage (V)	Power (W)	Current (A)	Current number
USB HUB	12	48.72	4.06	I_1
Jetson TX2	12	55.1	4.59	I_2
Front LiDAR	12	8	0.67	I_3
Rear LiDAR	12	8	0.67	I_4

$$I_s = I_1 + I_2 + I_3 + I_4 \tag{16}$$

$$I_s = 4.06\,A + 4.59\,A + 0.67\,A + 0.67\,A = \boldsymbol{9.99\,A} \tag{17}$$

This result indicates that the current required by the whole circuit is less than what the battery could supply. With this result, the theory number one would be discarded.

3. Considering 48 watts as the power dissipated by the CPU

According to the datasheet for the Jetson TX2 (Appendix A.4), with a main power input from DC Adapter (5.5 V – 19.6 V) the maximum current could be of 4 amperes (Table 10). Using this information, the power can be calculated as follows:

Table 10. Interface Supply Current Capabilities, [A.4].

Power Rails	Usage	(V)	Max Current (mA)
VDD_IN/VDD_MUX	Main power input from DC Adapter	5.5-19.6	~4000
VDD_5V0_IO_SYS	Main 5V supply	5.0	7000
VDD_3V3_SYS	Main 3.3V supply	3.3	7000
VDD_1V8	Main 1.8V supply	1.8	2000
VDD_12V_SLP	12V rail for PCIe x4 & SATA	12.0	2300
DVDD_CAM_IO_1V8	1.8V rail for camera I/O	1.8	1000
AVDD_CAM	High voltage rail for cameras	2.8	1000
DVDD_CAM_IO_1V2	1.2V rail for camera I/O	1.2	200

$$P = VI = 12\,V \times 4\,A = 48\,W \tag{18}$$

With this result, the values used to perform the calculation with 48 watts, are shown in Table 11. With these values, the following calculations were made.

Table 11. Considering 48 watts as the power dissipated by the CPU.

Component	Voltage (V)	Power (W)	Current (A)	Current number
USB HUB	12	48.72	4.06	I_1
Jetson TX2	12	48	4	I_2
Front LiDAR	12	8	0.67	I_3
Rear LiDAR	12	8	0.67	I_4

$$I_S = I_1 + I_2 + I_3 + I_4 \tag{19}$$

$$I_S = 4.06\ A + 4\ A + 0.67\ A + 0.67\ A = \mathbf{9.4\ A} \tag{20}$$

This result indicates that the current required by the whole circuit is less than what the battery could supply. With this result, the theory number one would be discarded.

4. Considering 29.4 watts as the power dissipated by the CPU

According to the datasheet for the Jetson TX2 (Appendix A.4), with a main power input from DC Adapter (5.5 V – 19.6 V) the maximum current would be of 4 amperes. However, the main power input from DC adapter was considered using 19.6 V. In the circuit that it is being use in this research project, the power supply was of 12 volts. Therefore, using the Rule of Three with the above values, the current for the Jetson TX2 with 12 V, was calculated as follows.

$$19.6\ V\ - 4\ A \tag{21}$$

$$12.0\ V - y$$

$$y = \frac{(12.0\ V\ \times 4\ A)}{19.6\ V} = 2.45\ A \tag{22}$$

Using the above information, the current power consumption for the Jetson TX2 was calculated as follows.

$$P = VI = 12\ V\ \times 2.45\ A = 29.4\ W \tag{23}$$

With this result, the values used to perform the calculation with 29.4 watts, are shown in Table 12. With these values, the following calculations were made.

Component	Voltage (V)	Power (W)	Current (A)	Current number
USB HUB	12	48.72	4.06	I_1
Jetson TX2	12	29.4	2.45	I_2
Front LiDAR	12	8	0.67	I_3
Rear LiDAR	12	8	0.67	I_4

$$I_s = I_1 + I_2 + I_3 + I_4 \tag{24}$$

$$I_s = 4.06\ A + 2.45\ A + 0.67\ A + 0.67\ A = \mathbf{7.85\ A} \tag{25}$$

This result indicates that the current required by the whole circuit is less than what the battery could supply. With this result, the theory number one would be discarded.

5. Considering 15 watts as the power dissipated by the CPU

According to the NVIDIA Developer Blog [26], 15 watts is the maximum energy consumption. Using the following equation, the current can be calculated.

$$I = \frac{P}{V} = \frac{15\ W}{12\ V} = 1.25\ A \tag{26}$$

With this result, the values used to perform the calculation with 15 watts, are shown in Table 13. With these values, the following calculations were made.

Table 13. Considering 15 watts as the power dissipated by the CPU.

Component	Voltage (V)	Power (W)	Current (A)	Current number
USB HUB	12	48.72	4.06	I_1
Jetson board TX2	12	15	1.25	I_2
Front LiDAR	12	8	0.67	I_3
Rear LiDAR	12	8	0.67	I_4

$$I_s = I_1 + I_2 + I_3 + I_4 \tag{27}$$

$$I_s = 4.06\ A + 1.25\ A + 0.67\ A + 0.67\ A = \mathbf{6.65\ A} \tag{28}$$

This result indicates that the current required by the whole circuit is less than what the battery could supply. With this result, the theory number one would be discarded.

6. Considering 7.5 watts as the power dissipated by the CPU

According to the NVIDIA Developer Blog [26], 7.5 watts is the typical energy usage. A table obtained from this webpage is shown in Table 14.

Table 14. Features of Jetson TX1 vs Jetson TX2, [26].

	NVIDIA Jetson TX1	NVIDIA Jetson TX2
CPU	ARM Cortex-A57 (quad-core) @ 1.73GHz	ARM Cortex-A57 (quad-core) @ 2GHz + NVIDIA Denver2 (dual-core) @ 2GHz
GPU	256-core Maxwell @ 998MHz	256-core Pascal @ 1300MHz
Memory	4GB 64-bit LPDDR4 @ 1600MHz	25.6 GB/s	8GB 128-bit LPDDR4 @ 1866Mhz	59.7 GB/s
Storage	16GB eMMC 5.1	32GB eMMC 5.1
Encoder*	4Kp30, (2x) 1080p60	4Kp60, (3x) 4Kp30, (8x) 1080p30
Decoder*	4Kp60, (4x) 1080p60	(2x) 4Kp60
Camera†	12 lanes MIPI CSI-2	1.5 Gb/s per lane	1400 megapixels/sec ISP	12 lanes MIPI CSI-2	2.5 Gb/sec per lane	1400 megapixels/sec ISP
Display	2x HDMI 2.0 / DP 1.2 / eDP 1.2	2x MIPI DSI	
Wireless	802.11a/b/g/n/ac 2×2 867Mbps	Bluetooth 4.0	802.11a/b/g/n/ac 2×2 867Mbps	Bluetooth 4.1
Ethernet	10/100/1000 BASE-T Ethernet	
USB	USB 3.0 + USB 2.0	
PCIe	Gen 2	1×4 + 1 x1	Gen 2	1×4 + 1×1 or 2×1 + 1×2
CAN	Not supported	Dual CAN bus controller
Misc I/O	UART, SPI, I2C, I2S, GPIOs	
Socket	400-pin Samtec board-to-board connector, 50x87mm	
Thermals‡	-25°C to 80°C	
Power††	10W	7.5W
Price	$299 at 1K units	$399 at 1K units

Table 1: Comparison of Jetson TX1 and Jetson TX2.
* Supported video codecs: H.264, H.265, VP8, VP9
† MIPI CSI-2 bifurcation: up to six 2-lane or three 4-lane cameras
‡ Operating temperature range, TTP max junction temperature.
†† Typical power consumption under load. input ~5.5-19.6 VDC. Jetson TX2: Max-Q profile.

Using the following equation, the current can be calculated.

$$I = \frac{P}{V} = \frac{7.5\ W}{12\ V} = 0.625\ A \tag{29}$$

With this result, the values used to perform the calculation with 7.5 watts, are shown in Table 15. With these values, the following calculations were made.

Table 15. Considering 7.5 watts as the power dissipated by the CPU

Component	Voltage (V)	Power (W)	Current (A)	Current number
USB HUB	12	48.72	4.06	I_1
Jetson board TX2	12	7.5	0.625	I_2
Front LiDAR	12	8	0.67	I_3
Rear LiDAR	12	8	0.67	I_4

$$I_s = I_1 + I_2 + I_3 + I_4 \tag{30}$$

$$I_S = 4.06\,A + 0.625\,A + 0.67\,A + 0.67\,A = \mathbf{6.025\,A} \qquad\text{(31)}$$

This result indicates that the current required by the whole circuit is less than what the battery could supply. With this result, the theory number one would be discarded.

After the above calculations were made, as most of them indicated that the current required by the whole circuit could be supplied by the battery, field tests were carried out.

A "truth table" was proposed to perform combinations of measuring power and current for the battery, switch, Jetson TX2 and both LiDAR sensors. After performing the measurements, results were registered in Table 16.

In Table 16, can be observed that the power for the Jetson TX2 (CPU in table) did not exceed 9.27 watts. According to the first calculation about this theory (theory number one), the maximum power should be 90 watts. When the measurements were performed, CPU reached 9.27 watts when everything was on and the software was running in its maximum performance, according to the project research specifications. Using the Rule of Three, it was determined that the power used by CPU corresponded to 10.3% of the maximum power consumption, according to the first calculation.

$$90\,W - 100\,\% \qquad\text{(32)}$$
$$9.27\,W - z$$

$$z = \frac{(9.27\,W \times 100)}{90\,W} = 10.3\% \qquad\text{(33)}$$

Table 16. Truth table - Measurements and combinations.

	A (USB HUB)	B (CPU)	C (FRONT LIDAR)	D (REAR LIDAR)	Battery (V)	Battery (A)	Battey (P)	Switch (V)	Switch (A)	Switch (P)	USB Hub (V)	USB Hub (A)	USB Hub (P)	CPU (V)	CPU (A)	CPU (P)	F. Lidar (V)	F. Lidar (A)	F. Lidar (P)	R. Lidar (V)	R. Lidar (A)	R. Lidar (P)	Total Components (A)
0	0	0	0	0	12.80	0.00	0.00	12.80	0.00	0.00	0.00	0.00	0.00	0.70	0.00	0.00	0.00	0.00	0.00	0.00	0.00	0.00	0.00
1	0	0	0	1	12.70	0.54	6.86	12.70	0.54	6.86	0.00	0.00	0.00	0.70	0.00	0.00	0.00	0.00	0.00	12.70	0.54	6.86	0.54
2	0	0	1	0	12.60	0.56	7.06	12.60	0.57	7.18	0.00	0.00	0.00	0.70	0.00	0.00	12.60	0.56	7.06	0.00	0.00	0.00	0.56
3	0	0	1	1	12.60	1.11	13.99	12.50	1.11	13.88	0.00	0.00	0.00	0.70	0.00	0.00	12.50	0.56	7.00	12.50	0.55	6.88	1.11
4	0	1	0	0	12.60	0.32	4.03	12.60	0.12	1.51	0.00	0.00	0.00	12.60	0.30	3.78	0.00	0.00	0.00	0.00	0.00	0.00	0.30
5	0	1	0	1	12.80	0.80	10.24	12.45	0.80	9.96	0.00	0.00	0.00	12.40	0.28	3.47	0.00	0.00	0.00	12.40	0.54	6.70	0.82
6	0	1	1	0	12.50	0.86	10.75	12.40	0.86	10.66	0.00	0.00	0.00	12.40	0.28	3.47	12.40	0.60	7.44	0.00	0.00	0.00	0.88
7	0	1	1	1	12.40	1.42	17.61	12.30	1.39	17.10	0.00	0.00	0.00	12.30	0.28	3.44	12.30	0.58	7.13	12.30	0.52	6.40	1.38
8	1	0	0	0	12.30	0.52	6.40	12.30	0.52	6.40	12.20	0.52	6.34	0.90	0.00	0.00	0.00	0.00	0.00	0.00	0.00	0.00	0.52
9	1	0	0	1	12.30	1.07	13.16	12.20	1.07	13.05	12.20	0.54	6.59	0.90	0.00	0.00	0.00	0.00	0.00	12.10	0.54	6.53	1.08
10	1	0	1	0	13.70	1.02	13.97	13.70	1.02	13.97	13.60	0.50	6.80	0.80	0.00	0.00	13.60	0.54	7.34	0.00	0.00	0.00	1.04
11	1	0	1	1	13.80	1.54	21.25	13.80	1.52	20.98	13.70	0.48	6.58	0.80	0.00	0.00	13.70	0.54	7.40	13.70	0.50	6.85	1.52
12	1	1	0	0	14.00	1.48	20.72	13.90	1.46	20.29	13.90	1.18	16.40	13.90	0.26	3.61	0.00	0.00	0.00	0.00	0.00	0.00	1.44
13	1	1	0	1	14.00	1.98	27.72	13.90	1.96	27.24	13.90	1.19	16.54	13.90	0.27	3.75	0.00	0.00	0.00	13.80	0.48	6.62	1.94
14	1	1	1	0	14.00	2.04	28.56	13.90	2.02	28.08	13.90	1.20	16.68	13.90	0.28	3.89	13.90	0.54	7.51	0.00	0.00	0.00	2.02
15	1	1	1	1	14.00	2.58	36.12	13.90	2.56	35.58	13.80	1.26	17.39	13.80	0.30	4.14	13.90	0.56	7.78	13.80	0.50	6.90	2.62
16	HOME				12.50	3.22	40.25	12.20	3.30	40.26	12.20	1.44	17.57	12.30	0.70	8.61	12.20	0.62	7.56	12.20	0.56	6.83	3.32
17	LIDAR				12.50	3.28	41.00	12.20	3.32	40.50	12.20	1.44	17.57	12.20	0.76	9.27	12.20	0.64	7.81	12.20	0.60	7.32	3.44
18	CAMERA - STEREO				12.50	3.32	41.50	12.20	3.31	40.38	12.20	1.42	17.32	12.20	0.74	9.03	12.20	0.58	7.08	12.20	0.56	6.83	3.30
19	CAMERA - DEPTH				12.40	3.36	41.66	12.20	3.24	39.53	12.10	1.38	16.70	12.10	0.70	8.47	12.20	0.58	7.08	12.20	0.54	6.59	3.20

7. Considering 9.27 watts as the power dissipated by the CPU

According to the information shown in Table 16, the measurement for power for the Jetson TX2 was of 9.27 W. Using the following equation, the current can be calculated.

$$I = \frac{P}{V} = \frac{9.27\ W}{12\ V} = 0.77\ A \tag{34}$$

With this result, the values used to perform the calculation with 7.5 watts, are shown in Table 17. With these values, the following calculations were made.

Table 17. Considering 55.1 watts as the power dissipated by the CPU.

Component	Voltage (V)	Power (W)	Current (A)	Current number
USB HUB	12	48.72	4.06	I_1
Jetson board TX2	12	9.27	0.77	I_2
Front LiDAR	12	8	0.67	I_3
Rear LiDAR	12	8	0.67	I_4

$$I_s = I_1 + I_2 + I_3 + I_4 \tag{35}$$

$$I_s = 4.06\ A + 0.77\ A + 0.67\ A + 0.67\ A = \mathbf{6.17\ A} \tag{36}$$

This result indicates that the current required by the whole circuit is less than what the battery could supply. With this result, the theory number one would be discarded.

According to the results obtained by the calculations and measurements performed, the following can be determined.

- *The current required by the whole circuit is less than the battery can supply. Therefore, the battery is able to supply the circuit without problems.*

- *The current required by the whole circuit, according to the measurements, is less than 30% that the battery can supply.*

- ***The theory number one was discarded***, *the problem of the computer shutting down was not due to lack of power by the battery.*

Statements and tests regarding theory number two

On July 24th, 2019 when the test phase was carried out, the weather in Dallas was of 30℃ (86°F) according to *AccuWeather's* website [27]. Due to that, the theory number two was that overheating could be causing it to shut down as a security measure, the datasheet of the Jetson board TX2 (Appendix A.4) was checked and it was found that the operating temperature range is of 0℃ to 50℃.

With this data, theory number two was increasing in probabilities of being the root cause of the shutting down problem.

Recreating this scenario was tried, however, due to the controlled temperature on the laboratory (21.1℃ or 70°F) this was not possible. Also, due to weather conditions (1℃ or 33.8°F) in Dallas on November 11th, 2019, recreating this scenario outside, was not possible.

A contributing factor to this problem was discovered. At the time of conducting the driving tests, the top deck of the dashboard was closed, as observed in the Figure 45.

Figure 45. Closed top deck of the dashboard.

This contributed to the theory of overheating. As it could be observed, if the top deck of the dashboard was closed, there was no ventilation, which means that all the heat dissipated by the Jetson board TX2 cannot escape from the Jetson board TX2 compartment. This caused the heat to be stored and overheating occurs.

To solve this issue, three options were proposed:

1) Remove the top deck of the dashboard.

2) Pierce the top deck of the dashboard, making a ventilation slit.

3) Driving with the top deck of the dashboard opened.

To justify the chosen option, the following pros and cons table (Table 18) was performed.

Table 18. Theory number two - Pros and cons.

Option	Pros	Cons
1	It allows a complete air flow by having one of its 4 sides (the upper one) fully discovered.	It could be dangerous if there was something (liquid, dust or another external agent), leaving the Jetson board TX2 without protection against them all the time. If overheating was not the root cause of the problem, the top deck of the dashboard must be replaced.
2	It allows a partial air flow by having one of its 4 sides (the upper one) perforated.	It could be dangerous if there was something (liquid, dust or another external agent) leaving the Jetson board TX2 without protection against them all the time. If overheating was not the root cause of the problem, the top deck of the dashboard must be replaced.
3	It would allow a partial air flow by having one of its 4 sides (the upper one) opened. If overheating was not the root cause of the problem, the top deck could be closed again.	It could be dangerous if there was something (liquid, dust or another external agent) leaving the Jetson board TX2 without protection against them once the car is being driven.

According to the previous information, the option number 3 was selected. To perform the driving tests with the top deck of the dashboard, a piece of cardboard was placed, with the intention of keeping the lid open while the car was driven. This action can be observed in the Figures 46-47.

Figure 46. Top deck of dashboard opened - front view.

Figure 47. Top deck of dashboard opened - side view.

With the purpose of determining that theory number two was correct, driving tests, with all the components running, was performed. The last time that tests were performed (July 24th, 2019) the Jetson board turned off approximately 7 to 10 minutes after the car had begun to be driven. This time (November 11th, 2019) the car was driven for about 25 to 30 minutes and the computer did not turned off. Images obtained using the default software of VLP-16 and ZED, are shown in Figures 48-51.

Figure 48. Images obtained by the front VLP-16 sensor and front ZED camera, inside a parking lot – section A.

Figure 49. Images obtained by the front VLP-16 sensor and front ZED camera, inside a parking lot – section B.

Figure 50. Images obtained by the rear VLP-16 sensor and rear ZED camera, inside a parking lot – section A.

Figure 51. Images obtained by the rear VLP-16 sensor and rear ZED camera, inside a parking lot – section B.

According to the results obtained by the adjustments and tests performed, the following can be determined.

- *The lack of a ventilation slit in the compartment of the Jetson TX2, caused that the heat dissipated by the computer was not able to leave the compartment, causing an encapsulation of the dissipated heat.*

- *The heat dissipated by the Jetson TX2 must be able to leave the compartment. Because of this, it is necessary to provide the compartment with a way to release stored heat.*

- *Due to the above, **theory number two was accepted**. As result, it was concluded that the problem of the computer shutting down was due to overheating in the Jetson TX2, which was stored in the Jetson TX2 compartment.*

According to previous statements, it was proposed and recommended to pierce the Jetson TX2 compartment cover, in order to have a ventilation duct. It is expected that with this ventilation duct, the heat dissipated by the Jetson TX2 will be able to leave the Jetson TX2 compartment. The release of this stored heat would prevent the recurrence of the shutting down failure.

A solution and preventive actions were proposed, obtaining as a final result, a successful performance of the failure analysis.

5 CONCLUSIONS

Through the performance calculations, measurements and tests mentioned above, it was possibly to determinate that:

- ✓ The battery meets the requirements requested by the electronic system implemented in the car, which means that the car is able to supply all the components connected in this electronic system.

- ✓ The problem of the computer shutting down was due to overheating in the Jetson TX2, which was stored in the Jetson TX2 compartment. It is recommended to pierce the Jetson TX2 compartment cover, in order to have a ventilation duct. Having this ventilation duct, will allow the heat dissipated by the Jetson TX2 to be released. The release of this stored heat will prevent overheating in the Jetson TX2 compartment, which will solve the problem of turning off the Jetson TX2.

According to the above statements, it was possible to determine what was the root cause of the electronic system failure. Once this was figured out, its solution was implemented in the testbed. This implementation allowed to get the results shown in the previous section.

After these implementations and performed tests, it was possible to conclude the following:

- ✓ The car is now able to be driven with all the components running.
- ✓ The car is now able to recognize objects such as people, buildings, and cars. This is thanks to the Velodyne LiDAR VLP-16 sensors.
- ✓ The car can record video, using ZED cameras, when it is in motion. Also, using these cameras, the car is capable to record video in depth mode.
- ✓ The technical phase is done, which enables the research project to continue to the next phase.

The installations and interconnections of components for the monitoring system, as well as the failure analysis performed, according to the objectives set for the technical phase, had a high impact on the development of the "*Retrofitting a Polaris GEM e6*" research project. Since it enables the research project to seek achieving the phases of computing, mechanical, and final testing. Now, it seeks to continue the development of the research project, in order to achieve the main objectives, set at the beginning of this project.

It can be concluded that this technical report was performed successfully.

6 REFERENCES

[1] D. J. Fagnant and K. Kockelman, "Preparing a nation for autonomous vehicles: opportunities, barriers and policy recommendations," *Elsevier,* 2015.

[2] D. Calef and R. Goble, "The allure of technology: How France and California promoted electric and hybrid vehicles to reduce urban air pollution," Springer Science, 2007.

[3] T. Harmon, G. Bahar and F. Gross, "Crash Costs for Highway Safety Analysis," U.S. Department of Transportation, New Jersey, 2018.

[4] Statista, Inc., "Statista," Statistics, 24 July 2019. [Online]. Available: https://www.statista.com/statistics/859950/vehicles-in-operation-by-quarter-united-states/. [Accessed 12 November 2019].

[5] Q. Li, F. Qiao and L. Yu, "Will Vehicle and Roadside Communications Reduce Emitted Air Pollution?," *International Journal of Science and Technology,* vol. 5, 2015.

[6] I. Wagner, "Statista," Statistics, January 2019. [Online]. Available: https://www.statista.com/statistics/196010/total-number-of-registered-automobiles-in-the-us-by-state/. [Accessed 12 November 2019].

[7] The University of Texas at Dallas, "Enviromental Affairs," University, [Online]. Available: https://www.utdallas.edu/ehs/rm/environmental-affairs/. [Accessed 13 November 2019].

[8] J. Ruths, "Justin Ruths," Personal blog, [Online]. Available: http://justinruths.com/. [Accessed 13 November 2019].

[9] O. Osemwenkha, E. Gonzalez, M. Jennings, C. Cruz, R. Vastano and C. Skevofilax, "Final Project Report - Autonomous Golf Cart," The University of Texas at Dallas, Dallas, 2018.

[10] B. Kopankiewitz, G. Matthews, A. Mitschke and T. Stanley, "Communications Platform for an Autonomous Vehicle," The University of Texas at Dallas, Dallas, 2019.

[11] J. J. Rooney and L. N. Vanden Heuvel, "Root Cause Analysis For Beginners," *Quality Progress,* vol. 7, pp. 45-53, 2004.

[12] SFNQAPI, LLC, "SNF Quality Assurance & Performance Improvement," [Online]. Available: https://www.snfqapi.com/resources/root-cause-analysis. [Accessed November 2019].

[13] C. A. Riesenberger and S. D. Sousa, "The 8D Methodology: An Effective Way to Reduce Recurrence of Customer Complaints?," World Congress on Engineering 2010, London, 2010.

[14] J. Mauss, V. May and M. Tatar, "Towards Model-based Engineering: Failure Analysis with MDS".

[15] N. Kavvadias, P. Neofotistos, S. Nikolaidis, K. Kosmatopoulos and T. Laopoulos, "Measurements Analysis of the Software-Related Power Consumption in Microprocessors.," in *Technology Conference*, Vail, Colorado., 2003.

[16] K. Natarajan, H. Hanson, S. W. Keckler, C. R. Moore and D. Burger, "Microprocessor Pipeline Energy Analysis," The University of Texas at Austin, Seoul, Korea, 2003.

[17] S. Diary, H. Ibrahim and I. Muhammed, "Using DTVS Technique for Microprocessor's Power and Thermal Management," Salahaddin University-Erbil (SU), Erbil, Kurdistán, 2018.

[18] R. L. Boylestad, Introductory Circuit Analysis, Mexico: PEARSON EDUCACIÓN, 2004.

[19] S. William and Z. Li, Electricity generation using wind power, London: World Scientific Publishing Co. Pte. Ltd., 2017.

[20] P. Srividyadevi, D. V. Pusphalatha and P. M. Sharma, "Measurement of Power and Energy Using Arduino," *Research Journal of Engineering Sciences,* vol. 2, no. 10, pp. 10-15, 2013.

[21] Polaris Inc., "Polaris GEM," Vehicles, [Online]. Available: https://gem.polaris.com/en-us/e6/. [Accessed 13 November 2019].

[22] Velodyne Lidar, Inc, "Velodyne Lidar," Depth sensors, 2019. [Online]. Available: https://velodynelidar.com/vlp-16.html. [Accessed 12 November 2019].

[23] Stereolabs, "STEREOLABS," Cameras, 2019. [Online]. Available: https://www.stereolabs.com/zed/. [Accessed 12 November 2019].

[24] NVIDIA Corporation, "NVIDIA Developer," Electronics, [Online]. Available: https://developer.nvidia.com/embedded/jetson-tx2. [Accessed 13 November 2019].

[25] GeChic Corporation, "GeChic," Displays, [Online]. Available: https://www.gechic.com/en-portable-touch-monitor-onlap1102i-overview.html. [Accessed 13 November 2019].

[26] NVIDIA Corporation, "NVIDIA Developer," Electronics, 7 March 2017. [Online]. Available: https://devblogs.nvidia.com/jetson-tx2-delivers-twice-intelligence-edge/. [Accessed 13 November 2019].

[27] AccuWeather, Inc., "AccuWeather," Weather, July 2019. [Online]. Available: https://www.accuweather.com/es/us/dallas-tx/75202/july-weather/351194. [Accessed 14 November 2019].

7 ACHIEVEMENTS

Due to the participation in the project research "*Retrofitting a Polaris GEM e6 for autonomy*" [A], in the Summer 2019, I was invited and selected as a speaker at the final presentation of results of the *UTD Dallas-Mexico Summer Research 2019 Program.*

In August 2019, I was selected as a speaker at the "*Congreso Internacional del XXIV Verano de la Investigación Científica y Tecnológica del Pacífico*" congress [B], held in Nuevo Vallarta, Nayarit. In this congress I exposed the results obtained during my scientific research stay in Summer 2019.

In October 2019, I was selected as a speaker at the "*Encuentro de Jóvenes Investigadores en el Estado de Chihuahua 2019*" event [C], where I participated, exposing the results obtained during my scientific research stay in Summer 2019.

[A] A. U. Valenzuela Moreno and J. Ruths, "Retrofitting a Polaris GEM e6 for autonomy," in UT Dallas-Mexico Summer Research 2019 Program, Dallas, 2019.

[B] A. U. Valenzuela Moreno y J. Ruths, «Retrofitting a Polaris GEM e6 for autonomy,» de Congreso Internacional del XXIV Verano de la Investigación Científica y Tecnológica del Pacífico, Nuevo Vallarta, 2019.

[C] A. U. Valenzuela Moreno and J. Ruths, "Retrofitting a Polaris GEM e6 for autonomy," in Encuentro de Jóvenes Investigadores en el Estado de Chihuahua 2019, Ciudad Juárez, 2019.

APPENDICES

APPENDIX A

Appendix A.1 – Polaris GEM – 2018 Owner's manual

2018
OWNER'S MANUAL
GEM e2
GEM e4
GEMe6
GEM eLXD
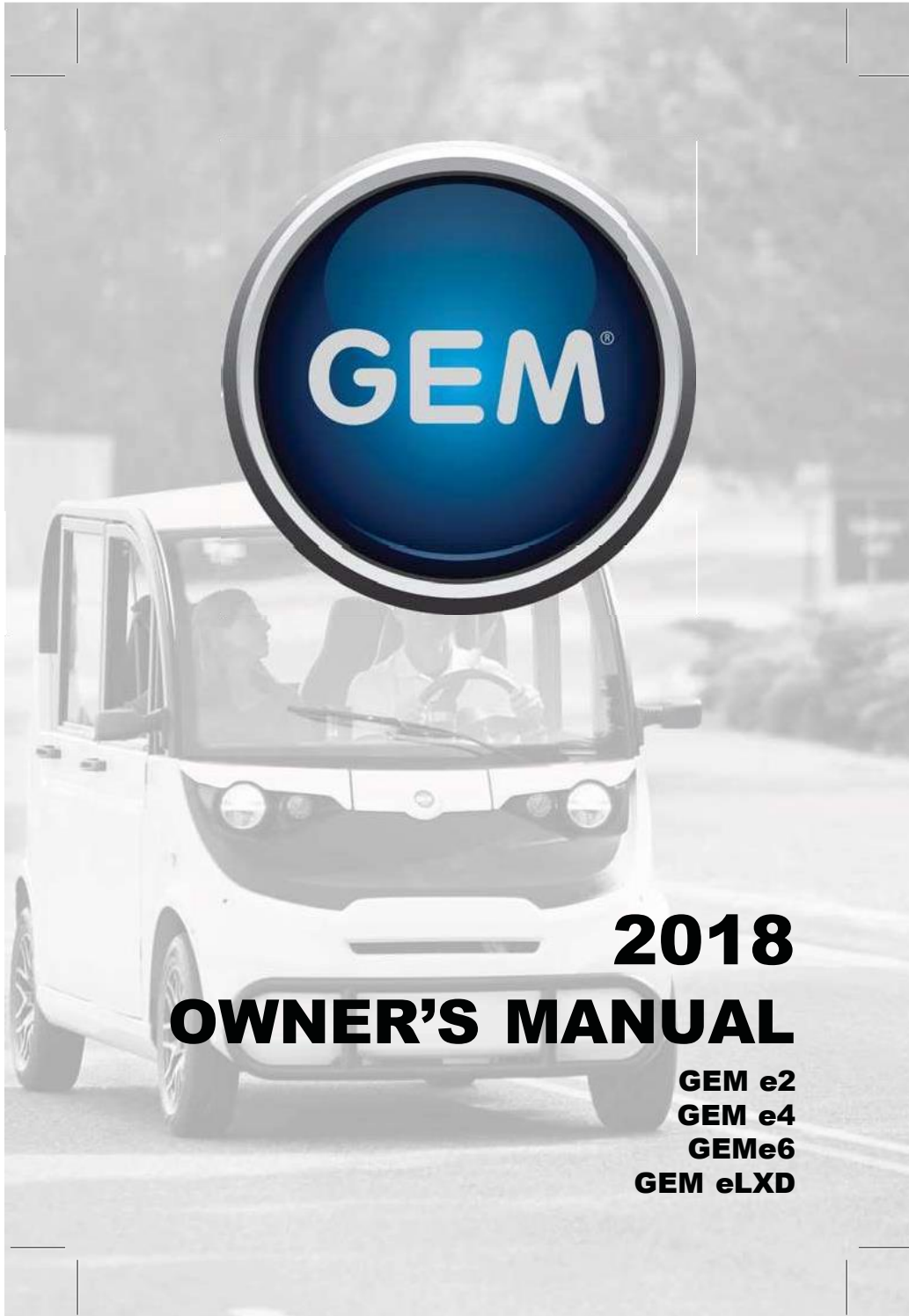
SPECIFICATIONS

	GEM E2	GEM E4
DIMENSIONS		
Dry Weight	1200 lbs. (544 kg)	1350 lbs. (612 kg)
Length	103 in. (262 cm)	135 in. (343 cm)
Width	55.5 in. (141 cm)	55.5 in. (141 cm)
Height	73.1 in. (186 cm)	73.1 in. (186 cm)
Wheelbase	69 in. (175 cm)	101 in. (257 cm)
Turning Circle/Radius	150 in. (381 cm)	207 in. (526 cm)
LOAD CAPACITY		
Payload Capacity (occupants, cargo, options)	800 lbs. (363 kg)	1150 lbs. (521.6 kg)
Gross Vehicle Weight Rating (GVWR)	2000 lbs. (907 kg)	1150 lbs. (521.6 kg)
Gross Axle Weight Rating (GAWR), Front and Rear	1280 lbs. (581 kg)	1600 lbs. (726 kg)
Seating	2	4
PERFORMANCE		
Motor	5 kW (optional 6.5 kW) AC electric	
Motor peak	13.3 kW (optional 18.5 kW)	
Controller	Sevcon 450A AC Controller	
Maximum speed	25 MPH (40 km/h)	
Range	Varies with conditions	
Drive System	17.05:1 Single speed	
On-board charger	Standard 1 kW, 120/240V input (optional 3 kW or 6 kW, SAE J1772)	

BRAKE SYSTEM	
Brakes	4-Wheel hydraulic brakes, disc front, drum rear
Park Brake	Dash-mounted lever-activated mechanical park brake
Front suspension	MacPherson Strut
Rear suspension	Independent w/coil over shock
Tires	14-inch Aluminum 4.5-inch ET11 165/70R14 This tire should only be replaced by a 165/70R14 81T tire
Tire pressure	35 psi (241 kPa)

	GEM EL XD	GEM E6®
DIMENSIONS		
Dry Weight	1585 lbs. (720 kg)	1696 lbs. (769 kg)
Length	145.5 in. (370 cm)	167 in. (424 cm)
Width	55.5 in. (141 cm)	55.5 in. (141 cm)
Height	73.1 in. (186 cm)	73.1 in. (186 cm)
Wheelbase	114 in. (289.6 cm)	133.5 in. (339 cm)
Turning Circle/Radius	233 in. (592 cm)	264 in. (671 cm)

LOAD CAPACITY		
Payload Capacity (occupants, cargo, options)	1415 lbs. (642 kg)	1304 lbs. (591 kg)
Gross Vehicle Weight Rating (GVWR)	3000 lbs. (1360.8 kg)	3000 lbs. (1360.8 kg)
Gross Axle Weight Rating (GAWR), Front and Rear	1920 lbs. (871 kg)	1920 lbs. (871 kg)
Seating	2	6

SPECIFICATIONS

PERFORMANCE	
Motor	6.5 kW AC electric
Motor peak	18.5 kW
Controller	Sevcon 450A AC Controller
Maximum speed	25 MPH (40 km/h)
Range	Varies with conditions
Drive System	17.05:1 Single speed
On-board charger	Standard 1 kW, 120/240V input (optional 3 kW or 6 kW, SAE J1772)

BRAKE SYSTEM	
Brakes	4-Wheel hydraulic brakes, disc front, drum rear
Park Brake	Console-mounted lever-activated mechanical park brake
Front suspension	MacPherson Strut
Rear suspension	Independent w/coil over shock
Tires	14-inch Aluminum 4.5-inch ET11 165/70R14 This tire should only be replaced by a 165/70R14 81T tire
Tire pressure	35 psi (241 kPa)

Velodyne LiDAR°

Puck™

REAL-TIME 3D LiDAR SENSOR

VLP-16

Velodyne LIDAR PUCK™

Velodyne's Puck (VLP-16) is the smallest, cost-optimized product in Velodyne's 3D LiDAR product range. Developed with mass production in mind, the Puck is far more cost-effective than comparable sensors, and it retains the key features of Velodyne's breakthroughs in LiDAR: Real-time, 360°, 3D distance and calibrated reflectivity measurements.

Real-Time 3D LIDAR

The VLP-16 has a range of 100 m, and the sensor's low power consumption, light weight, compact footprint and dual return capability make it ideal not only for autonomous vehicles but also for robotics, terrestrial 3D mapping and many other applications.

Velodyne's LiDAR Puck supports 16 channels, −300,000 points/second, 360° horizontal field of view and a 30° vertical field of view, with ±15° up and down. The Puck does not have visible rotating parts, and is highly resilient in challenging environments while operating over a wide temperature range.

DIMENSIONS *(Subject to change)*

OPTICAL CENTER

38.1mm 1.50in.

ACTIVE AREA FULL 360° 71.7mm 2.82in.

37.8mm 1.49in.

18.8mm 0.74in.

12.7mm MAX 0.50in. MAX

88.9mm 3.50in.

103.3mm Ø 4.07in.

12.7mm MAX 0.50in. MAX

12.7mm MAX 0.50in. MAX

2X Ø.16 FEATURES FOR 5/32in. PINS ↧ 7/32in. 5.5mm

90°

1/4-20 MOUNT ↧ 9/32in. 7.1mm

M12 CONNECTOR OPTION

ca. 56

M12

Ø20

PHOENIX CONTACT P/N: SACC-M12FS-8CON-PG 9-SH   18
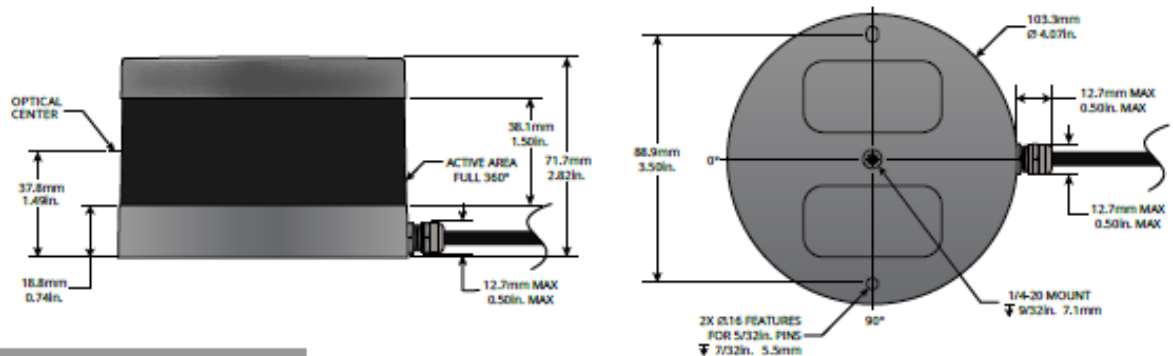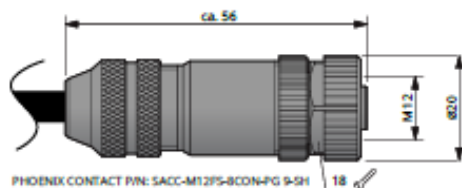
For other connector options contact
Velodyne Sales (sales@velodyne.com)

www.velodynelidar.com

VLP-16

Real-Time 3D LiDAR Sensor

The VLP-16 provides high definition 3-dimensional information about the surrounding environment.

	Specifications:
Sensor:	• 16 Channels • Measurement Range: 100 m • Range Accuracy: Up to ±3 cm (Typical)[1] • Field of View (Vertical): +15.0° to -15.0° (30°) • Angular Resolution (Vertical): 2.0° • Field of View (Horizontal): 360° • Angular Resolution (Horizontal/Azimuth): 0.1° – 0.4° • Rotation Rate: 5 Hz – 20 Hz • Integrated Web Server for Easy Monitoring and Configuration
Laser:	• Laser Product Classification: Class 1 Eye-safe per IEC 60825-1:2007 & 2014 • Wavelength: 903 nm
Mechanical/ Electrical/ Operational	• Power Consumption: 8 W (Typical)[2] • Operating Voltage: 9 V – 18 V (with Interface Box and Regulated Power Supply) • Weight: ~830 g (without Cabling and Interface Box) • Dimensions: See diagram on previous page • Environmental Protection: IP67 • Operating Temperature: -10°C to +60°C[3] • Storage Temperature: -40°C to +105°C

Output:	• 3D LiDAR Data Points Generated:
	    - Single Return Mode: ~300,000 points per second
	    - Dual Return Mode: ~600,000 points per second
	• 100 Mbps Ethernet Connection
	• UDP Packets Contain:
	    - Time of Flight Distance Measurement
	    - Calibrated Reflectivity Measurement
	    - Rotation Angles
	    - Synchronized Time Stamps (µs resolution)
	• GPS: $GPRMC and $GPGGA NMEA Sentences from GPS Receiver (GPS not included)

63-9229 Rev-H

For more details and ordering information, contact Velodyne Sales (sales@velodyne.com)

1. Typical accuracy refers to ambient wall test performance across most channels and may vary based on factors including but not limited to range, temperature and target reflectivity.
2. Operating power may be affected by factors including but not limited to range, reflectivity and environmental conditions.
3. Operating temperature may be affected by factors including but not limited to air flow and sun load.

⚠ CLASS 1 LASER PRODUCT

Appendix A.3 – ZED camera Detailed Specifications

—— **ZED** Detailed Specifications ——

Technical Specifications

Camera

Output Resolution	Side by Side 2x (2208x1242) @15fps
	2x (1920x1080) @30fps
	2x (1280x720) @60fps
	2x (640x480) @100fps
Output Format	YUV 4:2:2
Field of View	Max. 110° (D)
Depth Range	1 m to 15 m (3.5 to 49 ft)
Baseline	120 mm (4.7")
Interface	USB 3.0 - Integrated 1.5m cable

Electronics

Sensor Type	1/2.7"
Active Array Size	4M pixels per sensor
Focal Length	2.8mm (0.11") - f/2.0
Shutter	Electronic synchronized rolling shutter
Pixel Size	2µm

General

Dimensions	175x30x33 mm (6.89 x 1.18 x 1.3")
Weight	159g - 0.35 lb
Power	380mA / 5V USB Powered
Operating Temperature	0°C to +45°C (32°F to 113°F)

Mechanical Drawing
Dimensions are in mm

120 / 30 / 1/4"-20 Thread / 175
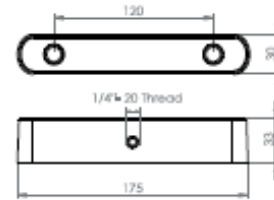
System Requirements

Windows 7, 8 and 10 - 64 bit
Linux (Ubuntu 12.04/14.04) - 64 bit
USB 3.0 or USB 2.0 port

ZED SDK Requirements
Dual-core 2.4GHz or faster processor
Minimum 4GB RAM
Nvidia GPU [1] 1GB Memory

(1) Compute capability ≥ 2.0
    Compatible with NVIDIA Tegra K1 an Tegra X1.

C++ Compiler:
Windows: Visual Studio 2012 or 2013
Linux: GNU Compiler collection (GCC)

Camera Control

The ZED is a UVC video camera with low level access to the device. Camera parameters such as frame rate, exposure time, white balance and gain can be controlled. ZED SDK also provides access to different resolutions such as side-by-side 1080p30, 720p60, VGA at 100fps, and a maximum resolution of 2208x1242 pixels at 15fps.

Use Case Diagram

ZED SDK

ZED Stereo Camera → Stereo Self Calibration → Depth Map → Point Cloud Fusion / Obstacle Detection / Visual Localization RGB-D SLAM → Automated Navigation

Laser, IMU, GPS

Left Video, Right Video

STEREOLABS www.stereolabs.com

Appendix A.4 – NVIDIA Jetson TX2 datasheet / NVIDIA Jetson TX1/TX2 Developer Kit
Carrier Board
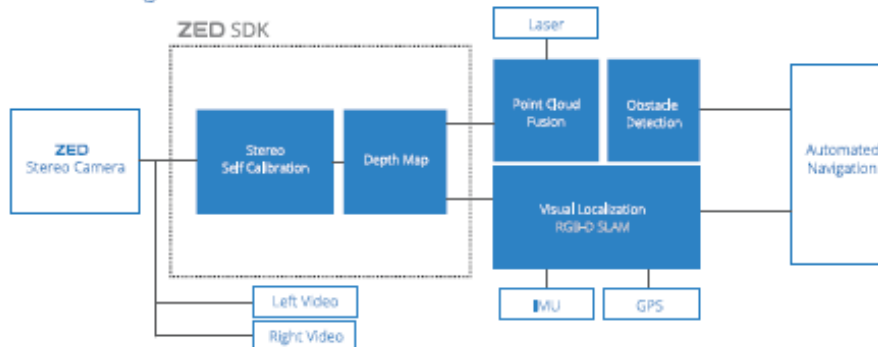
DATA SHEET [PRELIMINARY]

NVIDIA Jetson TX2 System-on-Module
Pascal GPU + ARMv8 + 8GB LPDDR4 + 32GB eMMC + WLAN/BT

Description

The NVIDIA® Jetson TX2 System-on-Module (SOM) redefines possibility; a combination of performance, power efficiency, integrated deep learning capabilities and rich I/O remove the barriers to a new generation of products. The Jetson TX2 is ideal for many applications including (but not limited to): Intelligent Video Analytics (IVA), Drones, Robotics, Gaming Devices, Virtual Reality (VR), Augmented Reality (AR) and Portable Medical Devices. Superior performance, robust design and reduced complexity in system integration results in more advanced products getting to market faster.

The Jetson TX2 module integrates:

- **256 core NVIDIA Pascal GPU.** Fully supports all modern graphics APIs, unified shaders and is GPU compute capable. The GPU supports all the same features as discrete NVIDIA GPUs, including extensive compute APIs and libraries including CUDA. Highly power optimized for best performance in embedded use cases.

- **ARMv8 (64-bit) Multi-Processor CPU Complex.** Two CPU clusters connected by a high-performance coherent interconnect fabric designed by NVIDIA; enables simultaneous operation of both CPU clusters for a true heterogeneous multi-processing (HMP) environment. The Denver 2 (Dual-Core) CPU clusters is optimized for higher single-thread performance; the ARM Cortex-A57 MPCore (Quad-Core) CPU clusters is better suited for multi-threaded applications and lighter loads.

- **Advanced HD Video Encoder.** Recording of 4K ultra-high-definition video at 60fps. Supports H.265 and H.264 BP/MP/HP/MVC, VP9 and VP8 encoding.

- **Advanced HD Video Decoder.** Playback of 4K ultra-high-definition video at 60fps with up to 12-bit pixels. Supports H.265, H.264, VP9, VP8 VC-1, MPEG-2, and MPEG-4 video standards.

- **Display Controller Subsystem.** Two multi-mode (eDP/DP/HDMI) outputs and up to 6-lanes of MIPI-DSI output. Multiple line pixel storage allows more memory-efficient scaling operations and pixel fetching. Hardware display surface rotation is also provided for bandwidth reduction in mobile applications.

- **128-bit Memory Controller.** 128-bit DRAM interface providing high bandwidth LPDDR4 support.

- **8GB LPDDR4 and 32 GB eMMC memory** integrated on the module

- **1.4Gpix/s Advanced Image signal processing:** Hardware accelerated still-image and video capture path, with advanced ISP.

- **Audio Processing Engine.** Audio subsystem enables full hardware support for multi-channel audio over multiple interfaces.

Description	Jetson TX2 System-on-Module*
Pascal GPU $^\diamond$	
256-core GPU	End-to-end lossless compression	Tile Caching	OpenGL® 4.5	OpenGL® ES 3.2	Vulkan® 1.0	CUDA® 8.0	GPGPU	
Maximum Operating Frequency	1.12GHz
CPU Complex ‡	
ARMv8 (64-bit) heterogeneous multi-processing (HMP) CPU architecture; two CPU clusters (6 processor cores) connected by a high-performance coherent interconnect fabric. NVIDIA Denver 2 (Dual-Core) Processor: L1 Cache: 128KB L1 instruction cache (I-cache) per core; 64KB L1 data cache (D-cache) per core	L2 Unified Cache: 2MB ARM® Cortex® -A57 MPCore (Quad-Core) Processor: L1 Cache: 48KB L1 instruction cache (I-cache) per core; 32KB L1 data cache (D-cache) per core	L2 Unified Cache: 2MB	

Maximum Operating Frequency per Core
  NVIDIA Denver 2
  ARM Cortex-A57
	
	2.0GHz
	2.0GHz

HD Video & JPEG	
Video Decode(Number of Streams Supported): H.265 [†]: Main 10, Main 8 H.265 [†]: Main 444 H.264 [†]: Baseline, Main, High H.264 [†]: MVC Stereo (per view) VP9 [†]: Profile 0 (8-bit) and 2 (10 and 12-bit) VP8: All MPEG1/2: Main MPEG4: SP/AP VC1: SP/MP/AP	(2x) 2160p60	(4x) 2160p30	(7x) 1080p60	(14x) 1080p30 2160p60	(2x) 2160p30	(3x) 1080p60	(7x) 1080p30 (2x) 2160p60	(4x) 2160p30	(7x) 1080p60	(14x) 1080p30 2160p60	2160p30	1080p60	1080p30 (2x) 2160p60	(4x) 2160p30	(7x) 1080p60	(14x) 1080p30 2160p60	(2x) 2160p30	(4x) 1080p60	(8x) 1080p30 2160p60	(2x) 2160p30	(4x) 1080p60	(8x) 1080p30 (4x) 1080p60	(8x) 1080p30 (2x) 1080p60	(4x) 1080p30

Video Encode (Number of Streams Supported):
  H.265
  H.264: Baseline, Main, High
  WEBM VP9
  WEBM VP8
	
	2160p60
		(3x) 2160p30	(4x)1080p60	(8x) 1080P30
				2160p60
					(3x) 2160p30	(7x) 1080p60	(14x) 1080p30
							2160p30
								(3x) 1080p60	(7x) 1080p30
									2160p30
										(3x) 1080p60	(6x) 1080p30

JPEG (Decode & Encode)	600 MP/sec
Audio Subsystem	
Industry-standard High Definition Audio (HDA) controller provides a multi-channel audio path to the HDMI interface	6 x I2S	4 x DMIC	2 x DSPK	SPDIF	2 x I and Q baseband data channels	PDM in/out	
Display Controller Subsystem	
Support for DSI, HDMI, DP and eDP	Two multi-mode eDP/DP/HDMI outputs.	

Captive Panel		
MIPI-DSI (1.5Gbps/lane)	Max Resolution	Support for Single x4 or Dual x4 links	2560x1600 at 60Hz
eDP 1.4 (HBR2 5.4Gbps)	Max Resolution	3840x2160 at 60Hz
External Display		
HDMI 2.0a/b (6Gbps)	Max Resolution	3840x2160 at 60Hz
DP 1.2a (HBR2 5.4 Gbps)	Max Resolution	3840x2160 at 60Hz

Imaging System	
Dedicated RAW to YUV processing engine process up to 1.4Gpix/s	MIPI CSI 2.0 up to 2.5Gbps (per lane)	Support for x4 and x2 configurations (up to 3 x4-lane or 6 x2-lane cameras)	
Clocks	
System clock: 38.4 MHz	Sleep clock: 32.768 KHz	Dynamic clock scaling and clock source selection	
Boot Sources	
Internal eMMC and USB (recovery mode)	

Description	Jetson TX2 System-on-Module*
Security	
Secure memory with video protection region for protection of intermediate results	Configurable secure DRAM regions for code and data protection	Hardware acceleration for AES 128/192/256 encryption and decryption to be used for secure boot and multimedia Digital Rights Management (DRM)	Hardware acceleration for AES CMAC, SHA-1, SHA-256, SHA-384, and SHA-512 algorithms	2048-bit RSA HW for PKC boot	HW Random number generator (RNG) SP800-90	TrustZone technology support for DRAM, peripherals	SE/TSEC with side channel counter-measures for AES	RSA-3096 and ECC-512/521 supported via PKA	
Memory ††	
128-bit DRAM interface	Secure External Memory Access Using TrustZone Technology	System MMU	
Memory Type	4ch x 32-bit LPDDR4
Maximum Memory Bus Frequency (up to)	1866MHz
Memory Capacity	8GB
Storage	
eMMC 5.1 Flash Storage	
Bus Width	8-bit
Maximum Bus Frequency	200MHz (HS400)
Storage Capacity	32GB
Connectivity	
WLAN	
Radio type	IEEE 802.11a/b/g/n/ac dual-band 2x2 MIMO
Maximum transfer rate	866.7Mbps
Bluetooth	
Version level	4.1
Maximum transfer rate	3MB/s
Networking	
10/100/1000 BASE-T Ethernet	IEEE 802.3u Media Access Controller (MAC)	Embedded memory	
Peripheral Interfaces ∆	
XHCI host controller with integrated PHY: (up to) 3 x USB 3.0, 3 x USB 2.0	USB 3.0 device controller with integrated PHY	5-lane PCIe: two x1 and one x4 controllers	SATA (1 port)	SD/MMC controller (supporting eMMC 5.1, SD 4.0, SDHOST 4.0 and SDIO 3.0)	5 x UART	3 x SPI	8 x I²C	2 x CAN	4 x I2S: support I²S, RJM, LJM, PCM, TDM (multi-slot mode)	GPIOs	
Temperature Specification	
Storage Temperature Range	-25C – 80C
Power Requirements ◆	
Power Input	5.5V – 19.6V
Applications	
Intelligent Video Analytics, Drones, Robotics, Industrial automation, Gaming, and more.	

* Refer to the software release feature list for current software support.

◊ GPU Maximum Operating Frequency: 1.3GHz supported in boost mode.
   Product is based on a published Khronos Specification and is expected to pass the Khronos Conformance Process. Current conformance status can be found at www.khronos.org/conformance.

‡ CPU Maximum Operating Frequency: 1-4 core = up to 2.0GHz; greater than 4 core = up to 1.4GHz

(†) For max supported number of instances: bitrate not to exceed 15 Mbps per HD stream (i.e., 1080p30), overall effective bitrate is less than or equal to 240 Mbps

†† Dependent on board layout. Refer to Interface Design Guide for layout guidelines.

∆ Refer to the Interface Design Guide and *Parker Series SoC Technical Reference Manual* to determine which peripheral interface options can be simultaneously exposed.

◆ Refer to the Product Design Guide and Thermal Design Guide for evaluating product power and thermal solution requirements

On SPECIFICATION

NVIDIA Jetson TX1/TX2 Developer Kit Carrier Board

Abstract

This document contains recommendations and guidelines for Engineers to follow to create modules for the expansion connectors on the Jetson™ carrier board as well as understand the capabilities of the other dedicated interface connectors and associated power solutions on the platform.

Note: Jetson TX2 utilizes Tegra X2 which is a Parker series SoC.

CAUTION:
1. ALWAYS CONNECT JETSON MODULE & ALL EXTERNAL PERIPHERAL DEVICES BEFORE CONNECTING THE POWER SUPPLY TO THE AC POWER JACK. Connecting a device while powered on may damage the Developer Kit carrier board, Jetson module or peripheral device. In addition, the carrier board should be powered down and the power removed before plugging or unplugging devices or add-on modules into the headers. Wait for the red power VDD_IN LED (See Figure 1) to turn off, or wait for 5 minutes if your system does not have a power LED. This includes the Jetson module, the camera & display headers, the M.2 connector, the PCIe® x4 connector, SATA & the other expansion headers. For the PCIex4 & SATA connector, also wait for the PCIe/SATA 12V LED to turn off (See Figure 1)

2. The NVIDIA® Jetson Developer Kit carrier board contains ESD-sensitive parts. Always use appropriate anti-static and grounding techniques when working with the system. Failure to do so can result in ESD discharge to sensitive pins, and irreparably damage your Jetson carrier board. NVIDIA will not replace units that have been damaged due to ESD discharge.

1.0 INTRODUCTION

The NVIDIA® Jetson Developer Kit carrier board is ideal for software development within the Linux environment. Standard connectors are used to access Jetson module features and interfaces, enabling a highly flexible and extensible development platform. (Jetson Developer Kits are not intended for production purposes.)

Go to https://developer.nvidia.com/embedded-computing for access to JetPack SDK. Use the JetPack installer to flash your Jetson Developer Kit with the latest OS image, to install developer tools for both host PC and Developer Kit, and to install the libraries and APIs, samples, and documentation needed to jumpstart your development environment.

1.1 Jetson Module Feature List

Applications Processor
- Tegra X1 or Tegra X2

Memory
- LPDDR4 DRAM & eMMC 5.1
- Memory sizes for DDR & eMMC vary depending on module — Check relevant Data Sheet

Network
- 10/100/1000 BASE-T Ethernet

Connectivity
- Dual U.FL RF connectors: Connects to 802.11a/b/g/n/ac WLAN/Bluetooth enabled devices.

Advanced power management
- Dynamic voltage and frequency scaling
- Multiple clock and power domains
- Thermal Transfer Plate & optional Fan/Heatsink

1.2 Carrier Board Feature List

Connection to Jetson Module
- 400-pin (8x50) Board-Board Connector

Storage
- Full Size SD Card Slot
- SATA Connector (Power & TX/RX)

USB
- USB 2.0 Micro AB (Host & Device)
- USB 3.0 Type A (Host only)

Wired Network
- Gigabit Ethernet (RJ45 Connector w/LEDs)

PCIe
- Standard PCIe® x4 connector

Display Expansion Header
- 120-pin (2x60) Board-Board
- DSI (2x4 lanes)
- eDP/DP/HDMI
- Backlight: PWM/Control
- Touch: SPI/I2C

HDMI Type A

Camera Expansion Header
- 120-pin (2x60) Board-Board
- CSI: 6, x2 — 3, x4
- Camera CLK, I2C & Control
- I2S, UART, SPI, Digital Mic (Jetson TX2 only)

M.2 Key E Connector
- PCIe x1 Lane, SDIO (Jetson TX1 only), USB 2.0
- I2S, UART, I2C, Control

Expansion Header
- 40-pin (2x20) header
- I2C, SPI, UART, I2S, Audio Clock/Control
- D-MIC (Jetson TX2 only)

GPIO Expansion Header
- 30-pin (2x15) header
- I2S, GPIOs, Digital Speaker (Jetson TX2 only)

UI & Indicators
- Power, Reset & Force Recovery Buttons
- LEDs: Main DC input, Main 3.3V (Power)/SOC Enables, M.2 Activity, PCIe/SATA 12V rail

Debug/Serial
- JTAG Connector (Standard 20-pin header)
- Debug Connector
  - 60-pin (2x30) Board-Board
  - JTAG, UART, I2C, Power, Reset & Recovery
- Serial Port Signals (1x6 header)

Miscellaneous
- Fan Connector: 5V, PWM & Tach

Power
- DC Jack: 5.5V-19.6V
- Main 3.3V/5V Buck Supplies: 2xTPS53015
- Main 1.8V Buck Supply: APW8805
- USB VBUS Load Switches: RT9715 & APL3511
- 12V Boost (PCIe & SATA): LM3481
- Load Switches/LDOs (SD/HDMI/Display/Camera)
- Charge Control Header: 10-pin Flex Receptacle

Developer Kit Operating Temperature Range
- 0ºC to 50ºC

The tables below show the allocation of supplies to the connectors on the Jetson carrier board and current capabilities.

Table 34 Interface Power Supply Allocation

Power Rails	Usage	(V)	Power Supply or Gate	Source	Enable
VDD_IN/VDD_MUX	Main power input from DC Adapter	5.5-19.6	FETs	DC Adapter	
VDD_5V0_IO_SYS	Main 5V supply	5.0	TPS53015	VDD_MUX	CARRIER_PWR_ON
VDD_3V3_SYS	Main 3.3V supply	3.3	TPS53015	VDD_MUX	3V3_SYS_BUCK_EN
VDD_1V8	Main 1.8V supply	1.8	APW8805	VDD_5V0_IO_SYS	1V8_IO_VREG_EN (VDD_3V3_SYS_PG)
VDD_3V3_SLP	3.3V rail, off in Sleep (various)	3.3	FETs	VDD_3V3_SYS	SOC_PWR_REQ
VDD_5V0_IO_SLP	5V rail, off in Sleep (SATA/FAN)	5.0	FETs	VDD_5V0_IO_SYS	SOC_PWR_REQ
VDD_12V_SLP	12V rail, off in Sleep (PCIe* x4 & SATA)	12.0	LM3481MMX Boost	VDD_5V0_IO_SYS	VDD_3V3_SLP
VDD_VBUS_CON	5V VBUS for USB 2.0 Type AB conn.	5.0	APL3511CBI Load Switch	VDD_5V0_IO_SYS	USB_VBUS_EN0
USB_VBUS	5V VBUS for USB 3.0 Type A conn.	5.0	RT9715 Load Switch	VDD_5V0_IO_SYS	USB_VBUS_EN1
SD_CARD_SW_PWR	SD Card power rail	3.3	APL3511DBI Load Switch	VDD_3V3_SYS	SDCARD_VDD_EN
VDD_5V0_HDMI_CON	5V rail for HDMI connector		RT9728 Load Switch	VDD_5V0_IO_SYS	5V0_HDMI_EN (GPIO Expander U32, P14)
VDD_TS_1V8	1.8V rail for touch screen		TPS22915 Load Switch	VDD_1V8	EN_VDD_TS_1V8_PMIC (GPIO Expander U32, P01)
AVDD_TS_DIS	High voltage rail for touch screen	3.3	TPS22915 Load Switch	VDD_3V3_SLP	EN_VDD_TS_HV_PMIC (GPIO Expander U32, P02)
VDD_LCD_1V8_DIS	1.8V rail for panel		TPS22915 Load Switch	VDD_1V8	VDD_LCD_1V8_EN (GPIO Expander U32, P11)
VDD_DIS_3V3_LCD	High voltage rail for panel		TPS22915 Load Switch	VDD_3V3_SYS	EN_VDD_DISP (GPIO Expander U32, P03)
VDD_1V2	Generic 1.2V display rail	1.2	TLV73312 LDO	VDD_1V8	DIS_VDD_1V2_EN (GPIO Expander U32, P12)
VDD_SYS_BL	Rail to LCD backlight driver	Device Dep.	Stuffing option Resistors	VDD_MUX VDD_5V0_IO_SYS	Na
DVDD_CAM_IO_1V8	1.8V rail for camera I/O	1.8	TPS22915 Load Switch	VDD_1V8	CAM_VDD_1V8_EN (GPIO Expander U31, P11)
AVDD_CAM	High voltage rail for cameras	2.8	APL5932	VDD_3V3_SLP	CAM_AVDD_CAM_EN (GPIO Expander U32, P15)
DVDD_CAM_IO_1V2	1.2V rail for camera I/O	1.2	TLV73312	VDD_1V8	CAM_VDD_1V2_EN (GPIO Expander U31, P12)

Table 35 Interface Supply Current Capabilities

Power Rails	Usage	(V)	Max Current (mA)
VDD_IN/VDD_MUX	Main power input from DC Adapter	5.5-19.6	~4000
VDD_5V0_IO_SYS	Main 5V supply	5.0	7000
VDD_3V3_SYS	Main 3.3V supply	3.3	7000
VDD_1V8	Main 1.8V supply	1.8	2000
VDD_12V_SLP	12V rail for PCIe x4 & SATA	12.0	2300
DVDD_CAM_IO_1V8	1.8V rail for camera I/O	1.8	1000
AVDD_CAM	High voltage rail for cameras	2.8	1000
DVDD_CAM_IO_1V2	1.2V rail for camera I/O	1.2	200

Notes:
1. When operated near the minimum voltage, the power supported by some of the supplies may be reduced.
2. The supplied power adapter is rated to 90W.
3. The values shown in the "Supported Current" column indicate the total power available on the expansion connectors (not per pin).
4. If a given voltage rail cannot provide enough current, a possible solution is for the user to use a regulator from VDD_5V0_IO_SYS, VDD_3V3_SYS or VDD_1V8 to generate the desired rail.

Appendix A.5 – Anker USB Hub Welcome Guide

Welcome Guide

AH241 USB 3.0 13-Port
+ 1 Smart Charging Port Aluminum Hub

Package Contents

- Anker AH241 USB 3.0 13-Port + 1 Smart Charging Port Aluminum Hub
- USB 3.0 cable (2.6ft)
- 12V 5A power adapter (10ft)
- Welcome guide

Features

- Easily add 13 USB 3.0 ports to any compatible system and eliminate the hassle of having to switch between devices.
- The Smart Charging Port enables full-speed charges (up to 2.1A) and universal charging compatibility.
- Save syncing time with data transfer rates of up to 5 Gbps (much faster than USB 2.0).
- Upwards-facing ports give wider berth for over-sized USB plugs.
- External power supply ensures multiple devices work simultaneously.
- Built-in surge protector keeps your devices and data safe and supports hot swapping.
- Compatible with USB 2.0 and 1.1 specifications; no driver required for Windows XP/Vista/7/8 and Mac OS 10.2 and above.

Specifications

Product Name	Anker AH241 USB 3.0 13-Port + 1 Smart Charging Port Aluminum Hub
Product Model	BW-U3039A
Color	Black
Material	Aluminum
Dimensions	195 × 46 × 26mm / 7.7 × 1.8 × 1.0 in(L × W × H)
Weight	215g / 7.6oz
Input Interface	USB 3.0 type B
Output Interface	13 type A USB 3.0 ports with maximum speeds of up to 5Gbps, 1 type A Smart Charging Port with output current of 2.1A.
Supported Systems	Windows 8 / 7 / Vista / XP or Mac OS X 10.2 and above.
Safety Approval	CE, FCC, RoHS

Instructions

Use the DC power adapter to connect the hub to a power outlet. Use the USB 3.0 type B cable to connect the hub to your computer. It's now ready to connect and charge your devices.

To achieve maximum performance, your computer system, peripherals, cables, and software must all support USB 3.0.

Usage Tips

1. For maximum performance, connected devices should not exceed a combined current of 8A. Otherwise, connections may become unstable or disconnect entirely.

   For reference, the devices below are often rated as:

Mouse	100mA
Camera	>300mA
Portable hard disk	max. 500mA
USB 3.0 portable hard disk	max. 900mA
Keyboard	max. 500mA

   (1000mA = 1A)

   The ratings above are estimates only. Please check your specific devices' ratings before connecting to the hub.

2. The Smart Charging Port has its own microchip that detects what device is plugged into it through USB pin signals. This enables it to charge each unique device at its fully-intended speed (up to 2.1A) without the risk of harming it. This port can't be used to transmit data.

3. 2.4 GHz wireless devices, such as wireless keyboards and mouse adapters, may not work in close proximity to USB 3.0 devices or hubs. Connecting to a USB 2.0 port is recommended.

4. Some USB 3.0 devices require a direct connection to host USB 3.0 ports, including some USB 3.0 hard disks.

NOTES

1. Do not tamper with this product or expose it to excessive heat, humidity, or direct sunlight.

2. Our company will not be held responsible for any damage to drives or hard drive data caused by improper use and/or disassembly. Please use this product according to its instructions.

On-Lap 1102

User Manual
ユーザーガイド

Let's Play with
On-Lap Monitor

GeChic Global

Chapter 6 Product Specification
Section 1 General Specification

Item	On-Lap1102E	On-Lap1102H	On-Lap1102I
Panel	Wide screen 11.6" (16: 9)	Wide screen 11.6" (16: 9)	Wide screen 11.6" (16:9)
True Resolution	1920x1080	1920x1080	1920x1080
Color Depth	16.7M colors	16.7M colors	16.7M colors
Brightness	300(cd/m²) (Typ.)	350 (cd/m²) (Typ.)	250 (cd/m²) (Typ.)
Contrast Ratio	1000:1(Typ.)	1000 : 1(Typ.)	1000:1(Typ.)
Viewing Angle	178°(H)/178°(V)(CR>10)	178°(H)/178°(V) (CR>10)	178°(H)/178° (V) (CR>10)
Response Time	12.5 (ms) (Typ.)	12.5 (ms) (Typ.)	12.5 (ms) (Typ.)
Type of Touchscreen Operating System	No Touch Function		Projective capacitive touch screen 10 points multi-touch Support Windows10/7
Connectivity	HDMI*2, VGA*1	HDMI*2, VGA*1	HDMI*2, VGA*1
Audio output	-	Earphone jack	Earphone jack
Speaker	1.0W(Max.)*2	1.0W(Max.)*2	1.0W(Max.)*2
HDCP Support	Yes	Yes	Yes
HDMI CEC Support	Yes	Yes	Yes
Plug and Play	VESA DDC2B/C1	VESA DDC2B/C1	VESA DDC2B/C1
Battery Type	-	Li-Polymer	-
Battery Capacity	-	6900mAh	-
Charge Time	-	3.5hr	-
.Power Consumption	≦ 8.5W	≦ 8.5W	≦ 8.5W
.Standby Mode	<0.5W	<0.5W	<0.5W
.Off Mode	<0.5W	<0.5W	<0.5W
Rating Power	5V ⋯ L.7A	5V ⋯ 1.7A	5V ⋯ 1.7A
Environment Condition	Operation: 0~50℃ Storage: -20~60℃		
Dimensions (W*H*D)	294mm*194mm*11mm (monitor) 299mm*209mm*21mm (monitor& cover)	294mm*194mm*11mm (monitor) 299mm*209mm*21mm (monitor& cover)	294mm*194mm*12mm (monitor) 299mm*209mm*21mm (monitor& cover)
Weight (typical)	490g(monitor) 740g(monitor& cover)	590g(monitor) 840g(monitor& cover)	670g(monitor) 920g(monitor& cover)
Certification	CE FC VCI RS3848 RoHS RoHS		
	-	CCC	CCC KC

APPLICATIONS

Southwire® SIM*pull* THHN® copper conductors are primarily used in conduit and cable trays for services, feeders and branch circuits in commercial or industrial applications as specified in the National Electrical Code. Voltage for all applications is 600 volts. SIM*pull* THHN® copper conductors are designed to be installed without application of a pulling lubricant.

These conductors have multiple ratings. Depending upon the product application, allowable temperatures are as follows:

- THHN or T90 Nylon- Dry locations not to exceed 90°C
- THWN-2- Wet or dry locations not to exceed 90°C or locations not to exceed 75°C when exposed to oil
- THWN- Wet locations not to exceed 75°C or dry locations not to exceed 90°C or locations not to exceed 75°C when exposed to oil
- TWN75- Wet locations not to exceed 75°C
- MTW- Wet locations or when exposed to oil at temperatures not to exceed 60°C or dry locations not to exceed 90°C (with ampacity limited to that for 75°C conductor temperature per NFPA 79)
- AWM- Dry locations not to exceed 105°C only when rated and used as appliance wiring material

STANDARDS & REFERENCES

Southwire® SIM*pull* THHN® copper conductors comply with the following:

- ASTM - B3, B8, and B787 (19 Wire Combination Unilay-Stranded)
- UL Standards 83, 758, 1063, and 1581
- CSA C22.2 No. 75, T90 Nylon/TWN75 Sizes through 1000 kcmil
- NOM-ANCE 90°C
- Federal Specification A-A-59544
- NEMA WC-70 (ICEA S-95-658) Construction Requirements
- National Electrical Code, NFPA 70
- CT Rated in Sizes 1/0 AWG and larger
- VW-1 - Sizes 14 through 1 AWG
- FT1 - All Sizes
- Sunlight Resistant – Sizes 2 AWG and larger
- AWM - Sizes 14 through 6 AWG
- MTW - Stranded Constructions Only
- RoHS/REACH Compliant

CONSTRUCTION

Southwire® SIM*pull* THHN® copper conductors are made with soft drawn copper. Sizes 14 through 4/0 AWG use a combination-unilay stranding while 250 kcmil and larger sizes use a compressed copper stranding. The wire is covered with a tough heat and moisture resistant PVC insulation with an overall nylon jacket utilizing SIM*pull*® Technology. Available in black, white, red, blue, purple, green, yellow, orange, brown, and gray. Also available in striped configurations. Some colors are subject to economic order quantity. Marked as THHN in all sizes. Also marked as THWN-2 in sizes 8 AWG and larger or marked as THWN in sizes 14, 12, and 10 AWG. Marked sunlight resistant in sizes 2 AWG and larger. Sizes 14, 12, and 10 AWG are available with SIM*pull*® Technology only in SIM*pull* BARREL™ cable drum or SIM*pull*® *Coil*PAK™ configurations.

Conductor		Insulation Thickness (mils)	Jacket Thickness (mils)	Nominal O.D. (mils)	Approx. Net Wt. Per 1000' (lbs.)	Allowable Ampacities+			Standard Package
Size (AWG or kcmil)	No. of strands					60°C	75°C	90°C	
14*	1	15	4	102	15	15	15	15	AC
12*	1	15	4	119	23	20	20	20	AC
10*	1	20	4	150	36	30	30	30	AC
14*	19	15	4	109	16	15	15	15	AC
12*	19	15	4	128	24	20	20	20	AC
10*	19	20	4	161	38	30	30	30	AC
8	19	30	5	213	63	40	50	55	ABCD
6	19	30	5	249	95	55	65	75	ABCD
4	19	40	6	318	152	70	85	100	ABCD
3	19	40	6	346	189	85	100	115	ABCD
2	19	40	6	378	234	95	115	130	ABCD
1	19	50	7	435	299	110	130	145	ABCD
1/0	19	50	7	474	372	125	150	170	ABCD
2/0	19	50	7	518	462	145	175	195	ABCD
3/0	19	50	7	568	575	165	200	225	ABCD
4/0	19	50	7	624	718	195	230	260	ABCD
250	37	60	8	694	851	215	255	290	ABCD
300	37	60	8	747	1012	240	285	320	ABC
350	37	60	8	797	1174	260	310	350	ABC
400	37	60	8	842	1334	280	335	380	ABC
500	37	60	8	926	1655	320	380	430	ABCD
600	61	70	9	1024	1987	350	420	475	ABC
750	61	70	9	1126	2464	400	475	535	BC
1000	61	70	9	1275	3257	455	545	615	C

* Sizes 14, 12, and 10 AWG are available with SIMpull® Technology only in SIMpull® Barrel or CoilPAK® configurations. Standard put ups vary from the ones shown on this chart for standard 14-10 AWG THHN.

+Allowable ampacities shown are for general use as specified by the 2014 Edition of the National Electrical Code Sections 310.15 and 240.4(D).

Unless the equipment is marked for use at higher temperatures the conductor shall be limited to the following per NEC 110.14(C):

60°C - When terminated to equipment for circuits rated 100 amperes or less or marked for 14 - 1 AWG conductors.

75°C - When terminated to equipment for circuits rated over 100 amperes or marked for conductors larger than 1 AWG.

90°C - THHN dry locations and THWN-2 wet or dry locations for ampacity adjustment purposes using NEC section 310.15.

Package Codes:
A - 2500' Reel
B - 1000' Reel
C - 500' Spool
D - 5000' Reel

Appendix A.8 – Extech 400 Series Multimeters

EX400 SERIES						

Specifications	EX410	EX411	EX420	EX430	EX450	EX470
Temperature (IR)	—	—	—	—	✓ -58 to 518°F (-50 to 270°C)	✓ -58 to 518°F (-50 to 270°C)
Averaging/True RMS	Averaging	✓ True RMS	Averaging	✓ True RMS	Averaging	✓ True RMS
Basic Accuracy (VDC)	±0.5%	±0.3%	±0.3%	±0.3%	±0.5%	±0.3%
AC Voltage	1mV to 750V	1mV to 750V	0.1mV to 750V	0.1mV to 750V	1mV to 750V	0.1mV to 750V
DC Voltage	0.1mV to 1000V	0.1mV to 1000V	0.1mV to 1000V	0.1mV to 1000V	0.1mV to 1000V	0.1mV to 1000V
AC Current	0.1mA to 20A	0.1mA to 20A	0.1μA to 20A	0.1μA to 20A	0.1μA to 20A	0.1μA to 20A
DC Current	0.1μA to 20A	0.1μA to 20A	0.1μA to 20A	0.1μA to 20A	0.1μA to 20A	0.1μA to 20A
Resistance	0.1Ω to 20MΩ	0.1Ω to 20MΩ	0.1Ω to 40MΩ	0.1Ω to 40MΩ	0.1Ω to 20MΩ	0.1Ω to 40MΩ
Capacitance	—	—	✓ 0.01nF to 100μF	✓ 0.01nF to 100μF	—	✓ 0.01nF to 100μF
Frequency	—	—	✓ 0.001Hz to 10MHz	✓ 0.001Hz to 10MHz	—	✓ 0.001Hz to 10MHz
Temperature (Type K)	-4 to 1382°F (-20 to 750°C)	-4 to 1382°F (-20 to 750°C)	-4 to 1382°F (-20 to 750°C)	-4 to 1382°F (-20 to 750°C)	—	-4 to 1382°F (-20 to 750°C)
Duty Cycle	—	—	✓ 0.1% to 99.9%	✓ 0.1% to 99.9%	—	0.1% to 99.9%
Continuity / Diode	Yes	Yes	Yes	Yes	Yes	Yes
Dimensions	7.4x3.2x2"(187x81x50mm)	7.4x3.2x2"(187x81x50mm)	7.4x3.2x2"(187x81x50mm)	7.4x3.2x2"(187x81x50mm)	7.4x3.2x2"(187x81x50mm)	7.4x3.2x2"(187x81x50mm)
Weight	0.75lbs (342g)	0.75lbs (342g)	0.75lbs (342g)	0.75lbs (342g)	0.75lbs (342g)	0.75lbs (342g)
Warranty	1 year	1 year	1 year	✓ 3 years	✓ 3 years	✓ 3 years

Appendix A.9 – 400A AC/DC CLAMP METER CL380

400A AC/DC AUTO-RANGING DIGITAL CLAMP METER

The CL380 is an automatically ranging true-root mean square (TRMS) digital clamp meter that measures AC/DC current via the clamp, AC/DC voltage, DC microamps, resistance, continuity, frequency, capacitance, tests diodes via test-leads, and temperature via a thermocouple probe. It features a high-visibility, reverse contrast LCD display that optimizes viewability both in dark or bright ambient lighting.

Measurement		CL380
AC/DC Voltage	V	600V
AC/DC Current	A	400A
Resistance	Ω	40MΩ
AC/DC Millivolts	mV	●
True RMS	TRMS	●
DC Microamps	μA	●
Non-Contact Voltage Testing	NCV	●
Audible Continuity	•)))	●
Temperature	°F°C	-40° – 1832°F (-40° – 1000°C)
Auto-Ranging	AUTO	●
Range Hold	RANGE	●
Data Hold	HOLD	●
Diode Test	►⊢	●
Capacitance Test	⊣⊢	●
Frequency/Duty Cycle	Hz%	●
Max/Min Value	MAX MIN	●
Relative Mode	△	●
Auto Power-Off	APO	●
LCD Display Count		4000 Reverse Contrast
Durability		
Safety Rating	△	CAT III 600V

Non-Contact Voltage Testing Sensor

Hold/Display Brightness Button

Clamp Trigger

Function Selector Switch

Function Buttons

LCD Reverse Contrast Display

Includes:
- Owner's Manual
- Carrying Case
- Test Leads
- Thermocouple Probe
- 3 x AAA Batteries

Test Lead/K-Type Thermocouple Input Jacks

Cat. No.	UPC# 0-92644+	Description	Height	Weight (with Batteries)
CL380	69172-0	400A AC/DC Auto-Ranging Digital Clamp Meter	8.66" (220 mm)	9.88 oz. (280 g)

See our complete line of Test & Measure products
www.kleintools.com

© 2019 Klein Tools, Inc.
Lincolnshire, IL 60069-1419
#2818 Rev. 02/19 A